Research in Context paper

Reappraisal of *Pseudobornia ursina* Nathorst: Implications for the evolution and systematics of Paleozoic sphenophytes

Alexis Rastier[1*], Eliott Capel[1], Valentin Fischer[1], Cyrille Prestianni[1]

[1] Evolution & Diversity Lab, Université de Liège, Allée du Six-Août, B18, Sart Tilman, 4000 Liège, Belgium.

*Corresponding author; A.Rastier@uliege.be

Abstract

Background and Aims

Sphenophytes, now restricted to *Equisetum*, were more diverse during the Paleozoic, particularly within Carboniferous coal swamp ecosystems. Despite their significance, the origins and phylogenetic relationships of sphenophytes with stem-group monilophytes remain poorly understood. In this context, the extinct order Pseudoborniales, typified by *Pseudobornia ursina* (Nathorst, 1894) from the Late Devonian of Bjørnøya (Norway), plays a key role in understanding the group's origin. However, conflicting interpretations of its reproductive structures have hindered its phylogenetic placement. Here, we provide a new description and reconstruction of the reproductive structures of *P. ursina* to evaluate its phylogenetic relationships with other sphenophytes and closely-allied groups, as well as to provide an updated perspective on the evolution of key traits among sphenopsids.

Methods

Fossils from the type locality were re-examined to clarify the morphology of the strobilus and fertile appendages. Comparative analyses were conducted with members of Sphenophyllales, Equisetales, and stem-group monilophytes. Phylogenetic relationships were assessed using parsimony and Bayesian methods.

Key Results

The strobilus of *P. ursina* displays distinctive features: (1) stalked, sporangia-bearing appendage, (2) oblique insertion of these structures in the bract axil, (3) ~30 erect sporangia

arranged on a wide-obconical receptacle, and (4) deeply bisected bracts with entire margins and parallel venation. Vegetative characters suggest equisetalean affinities, while reproductive traits more closely resemble stem sphenopsids. This mosaic points to a unique combination of ancestral traits within Sphenopsida, and phylogenetic analyses place *P. ursina* within Equisetales.

Conclusions

Our reappraisal of the strobilus of *Pseudobornia ursina* clarifies both its morphology and its phylogenetic placement, being recovered as part of stem Equisetales, sister to Archaeocalamitaceae. This suggests an evolutionary scenario where fertile appendages of stem sphenophytes became more compact over time, with either a fusion to a bract or the development of fertile internodes, combined to the loss of the bract, leading to the two main clades of Sphenophytes (Sphenophyllales and Equisetales).

Keywords: Devonian, Famennian, Bjørnøya, Bear Island, Equisetales, *Pseudobornia*, Sphenopsida, phylogeny

INTRODUCTION

Extant species of *Equisetum*, commonly known as horsetails, are the last surviving members of the once diverse clade Sphenopsida (Neuberg, 1964), defined by a whorled taxis, a ribbed stem and a highly regular and prominent segmentation into nodes and internodes. This evolutionary lineage can be traced back as early as the Late Devonian with representatives such as *Rinistachya* (Prestianni & Gess, 2019), *Xihuphyllum* (Huang *et al.*, 2017a), *Hamatophyton* (Li *et al.*, 1995; Wang *et al.*, 2006; Wang & Guo, 2009), and *Pseudobornia* (Nathorst, 1894). Nonetheless, it is during the Carboniferous period that sphenopsids achieved their highest diversity, representing one of the main components of the widespread coal swamp vegetation (Taylor *et al.,* 2009).

This group is traditionally divided into three main orders: Equisetales, Sphenophyllales, and Pseudoborniales (Nathorst, 1902; Boureau, 1964; Stein *et al.*, 1984; Stewart & Rothwell, 1993; Taylor *et al*., 2009). The two former groups are known to exhibit an important phenotypic disparity with both arborescent and herbaceous hygrophilous plants within the Equisetales and a dominance of herbaceous and liana habits within Sphenophyllales. Equisetales differed from the latter through the presence of (1) an equisetostele, and (2) exhibiting fertile phytomers producing fertile appendage whorls along internodes (Tomescu *et al*, 2017; Elgorriaga *et al.*, 2018).

Few studies have explored the phylogeny of sphenopsids in depth, and none have resolved the relationships within Sphenophyllales and stem sphenophytes (Skog & Banks, 1973; Stein *et al*., 1984; Elgorriaga *et al.*, 2018). Anatomical evidence suggests that Sphenophyllales form a monophyletic group, inheriting a ribbed protostele (actinostele) from iridopteridalean cladoxylopsids, while Equisetales evolved an equisetostele from the dissected steles of Cladoxylales and Pseudosporochnales, rendering Sphenopsida polyphyletic (Skog & Banks, 1973; Stein *et al.*, 1984). Sphenophyllalean fertile traits include nodal insertion of bract-

associated fertile appendages, whereas Equisetales lack partially fused or subtending bracts and bear peltate sporangiophores inserted along internodes (Boureau, 1964; Tomescu *et al*, 2017). Thus, fertile structures also differed significantly between Sphenophylalles and Equisetales, making it challenging to link the two lineages. In that respect, if the sphenophytes constitute a monophyletic group as suggested by Stein *et al*. (1984), stem sphenopsids might have originally exhibited a mosaic of characters combining equisetalean and sphenophyllalean traits prior to their divergence in the Mississippian, as well as plesiomorphic features inherited from Cladoxylopsida *sensu* Berry & Stein (2000). Although the whorled taxis appeared earlier in Emsian or even in putative late Lochkovian-early Pragian euphyllophytes (Chu *et al*., 2024; Tomescu and Whitewoods, 2024), Iridopteridales were recently proposed as a link between cladoxylopsids and Late Devonian sphenophytes, as they were among the first euphyllophytes to display a whorled taxis (Berry *et al*., 2022). Indeed, the whorled taxis is widely considered along with a pronounced morphological contrast between well-defined nodes and elongated internodes, forming an articulate stem pattern, a major synapomorphy linking Equisetales and Sphenophyllales. However, the scarcity of whole-plant concepts for early Sphenophyllales and the near-absence of equisetalean plants in the Late Devonian complicate the assessment of their affinities and the evolutionary scenarios of Stein *et al*. (1984).

The incompleteness of the fossil record and the challenges in interpreting morphological data in early sphenophytes also extends to the third order (i.e., the Pseudoborniales), established by Nathorst (1902) based on the type species *Pseudobornia ursina* (Nathorst, 1894, 1902) recovered in the Uppermost Famennian deposits on Bear Island (Norway). While this taxon is represented by abundant vegetative remains, only a single strobilus has ever been found. Moreover, conflicting morphological interpretations of this structure has led to significant uncertainties regarding the organisation of the fertile parts (Gothan and Weyland, 1973; Schweitzer, 2006). Consequently, *Pseudobornia* was excluded from most major systematic

studies of sphenophytes, despite its key temporal occurrence (Boureau, 1964; Orlova and Jurina, 2014).

In the 1960s, the single known strobilus of *Pseudobornia*, originally housed at the Naturhistoriska Riksmuseet in Stockholm (Sweden) as part of the Nathorst collections, was loaned to the University of Liège (Belgium) for research. Dr. Suzanne Leclercq (U. Liège) had the opportunity to study in detail this fertile specimen and proposed a preliminary morphological interpretation of a fertile node (Gothan and Weyland, 1973). The fertile node stands as loose fertile appendages bearing clustered erect sporangia, protected by a cupule-like structure and attached adaxially to the bract axil *via* a short stalk (Gothan and Weyland, 1973). H.J. Schweitzer strongly disagreed with this reconstruction and proposed, based on Nathorst's original line drawings and descriptions (Nathorst, 1894, 1902), his own interpretation with *Lilpopia*-like short-stalked globose fertile appendages adaxially inserted in the bract axil (Schweitzer, 2006). Unfortunately, this unique fossil was subsequently lost, and no further fertile specimens have been found to resolve the conflicting views. Orlova and Jurina (2014) later described another species, *P. schweitzeri*, from Frasnian deposits in Northern Timan (Russia), solely based on fragmentary vegetative remains. Fortunately, the original strobilus of *P. ursina* was recently rediscovered in the collections of the University of Liège (Belgium), enabling a new thorough description of the fertile remains.

Thus, in this study, we (I) redescribe the morphology of the fertile structures and vegetative remains of *P. ursina*; (II) propose a revised reconstruction of the fertile axes; and (III) assess the phylogenetic position of *P. ursina* within sphenophytes and closely related plant groups. Lastly, a discussion is thereafter provided on the vegetative and fertile trait acquisition sequence, providing new insights into sphenopsid morphological evolution.

MATERIALS AND METHODS

All specimens of *Pseudobornia ursina* in the Stockholm collection were collected on Bear Island, the southernmost island of the Norwegian Svalbard Archipelago in the Barents Sea (Fig. 1A-B). Nathorst (1894, 1902) and Antevs (Antevs & Nathorst, 1917) first collected material at Kolbukta (= coal bay), whilst further material was collected in subsequent expeditions by Hans-Joachim Schweitzer on Bear Island's northeastern coast, also at Kolbukta (Fig. 1B; Schweitzer, 1967, 1990, 2003, 2006). This material originates from the Late Devonian-early Tournaisian (Carboniferous) Røedvika Formation which extends up to 360 m thick along Bear Island's eastern coast (Fig. 1C). Four local Late Famennian-early Tournaisian subdivisions were defined within this formation: the Vesalstranda, Kapp Levin and Tunheim members (Cutbill & Challinor, 1965; Worsley & Edwards, 1976) and the Billefjorden Group (Worsley & Edwards, 1976; Dallmann *et al*., 1999; Worsley *et al*., 2001). *P. ursina* vegetative and fertile remains were solely found in the Tunheim Member exposed at Kolbukta (Fig. 1B). The latter features a root layer and thick coal seams, indicative of a vegetated floodplain (Worsley et al., 2001). This depositional pattern suggests a latest Famennian to early Tournaisian high sinuosity meandering fluvial system, with point bar deposits and a precursory coal swamp (Worsley & Edwards, 1976; Dallmann *et al*., 1999; Worsley *et al.*, 2001). The riverbanks and floodplain likely supported a diverse wetland flora, including previously described isoetalean lycopsids such as *Cyclostigma kiltorkense* and *Pseudolepidodendropis carneggianum,* alongside *P. ursina* (Sphenopsida) (Schweitzer, 2006).

The studied material of *P. ursina* is currently housed within the collections of the Naturhistoriska Riksmuseet (Stockholm, Sweden). These specimens exclusively consist of adpressions of vegetative organs, including leaves, branches of various orders and the main stem. The only known fertile specimen (S038066) figured as a drawing by Nathorst (1902, pl. XI, fig. XX), initially thought to be lost, was rediscovered in the collections of the University

of Liège (Belgium) by one of us (C.P.). During the study, another fertile specimen has been identified in the Antevs collections (S038344), originally recovered during the Swedish polar expedition of 1916, conducted by A.G. Nathorst and his student Ernst Valdemar Antevs, at Kolbukta and Engelska Staur (Bjørnøya). It originates from the same coal-bearing stratigraphic unit (Tunheim member) as the original material discovered by A.G. Nathorst (Antevs & Nathorst, 1917).

Both vegetative and fertile structures were examined and photographed using Panasonic LUMIX G100 and Canon R8 cameras with a lens Canon 100mm macro, under two LED lightboxes with polarised white light to acquire a maximum of morphological details. Ethanol was used on the fertile material to enhance the contrast because of its excellent refraction index (see Kerp & Bomfleur (2011) for additional methods on photographing fossil plants). *In situ* spores from the counterpart of the fertile specimen (sp. b) were extracted and macerated in the 1960s by Pr. Maurice Streel (U. Liège). Initial spore samples were collected from the sediments surrounding the strobili, followed by direct sampling from a *P. ursina* sporangium. Microscopic slides containing these spores were analysed using a Zeiss Axioskop transmitted light microscope and documented with a Zeiss Axiocam digital camera. They are currently housed in the paleobotanical collections of the University of Liège.

All the fossil materials examined in detail for this study are currently housed in the Swedish Museum of Natural History, within the Palaeobotanical collections located in the ground and first floors of the department of palaeobiology, including the original fertile axes of *Pseudobornia*, which has a Swedish collection number (S038066). Although this specimen was temporarily kept in the research facilities of the EDDy Lab (University of Liège) during the course of the study, it was returned to the Swedish Museum of Natural History in October 2025. The collection numbers of the specimens figured in the present work are: JE-Sch0067-01, JE-

Sch0071, JE- Sch0077, JE-Sch0181, S021000, S038344, S038050, S038054, S038058, S038068. Collection numbers beginning with "JE" are referring to specimens of the Schweitzer collection that are in a permanent loan. Therefore, they do not belong to the Swedish Museum of Natural History. Conversely, those that start with the letter "S" are specimens belonging to the Swedish Museum (Nathorst and Antevs collections).

Although the vegetative organs of *Pseudobornia ursina* were already described by A.G. Nathorst and H.J. Schweitzer, we also propose, alongside the study of the fertile specimen, a redescription of selected vegetative axes and leaves of *P. ursina* in order to highlight the main vegetative features of this plant and ultimately to perform a new phylogenetic analysis of sphenophytes involving *Pseudobornia ursina*.

Terminology of fertile organs

To ensure consistency and clarity in our descriptions and interpretations of sphenopsid fertile structures, a glossary of descriptive terms used throughout this study was established. This list is accompanied by an explanatory diagram, illustrating the main morphological characteristics observed in both sphenophytes and pseudosporochnalean cladoxylopsids (Fig. 2).

Bract: a leaf (or leaf-like structure) that bears a fertile appendage in its axil or in some cases, is partially fused with it (e.g, in Bowmanitaceae).

Fertile appendages: organs bearing reproductive structures, such as sporangia or seeds. These contrast with vegetative appendages, which typically includes leaves or sterile branches.

Receptacle: the tip of a stalk, often inflated and holding attached fertile structures (in this study, sporangia).

Shield and sporangiophore shield: a layer of thick-walled cells that covers and protects the sporangia (Bateman, 1991). This structure is conspicuous among the equisetalean fertile appendages (sporangiophores). A comparable shield is also observed in some Sphenophyllales like *Peltastrobus, Lilpopia* and in a lower extent in the genus *Bowmanites*. However, the shield is constrained to individual stalks in the latter group, not the entire fertile appendage.

Sporangiophore: a specialised appendage bearing sporangia. In most sphenopsids, sporangiophores are best interpreted as highly modified (reduced, fused) fertile branching systems. "Sporangiophore" is however often used for the specialised and highly reduced fertile appendage of Equisetales. Thus, to avoid any implied homology using this term, a more neutral word is favored here and throughout the paper, which is 'fertile appendage'.

Stalk: axial organ that bears fertile organs (e.g., sporangia, seeds).

Phylogenetic Analyses

Phylogenetic analyses were based on a new matrix including 29 taxa and 56 discrete morpho-anatomical characters (Table S1) compiled in Mesquite v3.81 (Maddison & Maddison, 2009). Character selection was informed by literature review, direct fossil observations, and previous phylogenetic analyses of Equisetales (Elgorriaga *et al*., 2018) and cladoxylopsids (Durieux *et al*., 2021). Among these 56 characters, 3 characters are ordered (Char. 8, 33 & 34), 19 are new, 12 are modified and 25 are similar or comparable to previously published matrices (Rothwell,

1991; Elgorriaga *et al*., 2018; Durieux *et al.*, 2021) (Appendix S1). Given the emphasis on reproductive morphology, taxa lacking described fertile structures (e.g., *Xihuphyllum megalofolium* (Huang *et al.*, 2017a) were excluded. *Psilophyton dawsonii* (Banks, Leclercq & Hueber, 1975) was designated as the outgroup. Parsimony-based phylogenetic analyses were conducted in TNT v1.5 (Goloboff & Catalano, 2016) under equal and extended implied weighting (k = 3, 6, 9 and 12). For both equal and implied weights, heuristic searches were performed using the extended search option (xmult), which combines sectorial searches, tree drifting and ratchet perturbations, with 10 replications. Tree bisection-reconnection (TBR) branch swapping was applied during the search. To construct maximum parsimonious trees (MPT), all branches supported ambiguously were collapsed following the tree-collapsing rule 1. Symmetric resampling (Goloboff *et al.*, 2003) with 10,000 replicates (P=33) was used for both equal and implied-weighting approaches. *A posteriori* time-scaling of the consensus tree was computed in R version 4.2.1 (R Core Team, 2022) using the timePaleoPhy and geoscalePhylo functions from the paleotree (Bapst, 2012) and strap (Bell & Lloyd, 2015) packages. First and last occurrence data (FAD/LAD) used for time-scaling are listed in Table S2, with corresponding references.

A Bayesian inference of phylogeny was conducted in MrBayes v3.2.7a (Huelsenbeck & Ronquist, 2001) using a maximum likelihood model for discrete morphological characters (Lewis, 2001). Four independent runs of 10 million generations were performed, discarding the first 25% as burn-in. The analysis produced an Estimated Sample Size (ESS) of 339.1, exceeding the threshold of 100, indicating sufficient sampling. The Potential Scale Reduction Factor (PSRF) of 1 confirmed convergence between runs. A relaxed morphological clock was implemented under an independent gamma rate model with fossil-tip sampling and a fossilized birth-death prior (FDB). Clock rates followed a lognormal distribution (SD = 0.5, mean = 0.006), calculated as the number of steps in the most parsimonious trees (141) divided by total

evolutionary duration (407 Myr) and number of characters (56), with a log transformation applied. Supporting values at nodes correspond to posterior probabilities. See supplementary information for the TNT, MrBayes and R scripts employed (Appendix S1) and for the historical taxonomy at the order level for each species involved in the phylogenetic analyses (Table S3).

RESULTS

Descriptions

Vegetative axes: stems, leaves, and whorled taxis

Specimens of *Pseudobornia ursina* originating from the Nathorst, Antevs and Schweitzer collections consist of multiple adpressions of axes, leaves and stem remains, rarely found in connection with one another (Fig. 3).

Trunk-like stems or first order axis of the specimens S038058, JE-Sch0071 and JE-Sch0181 in the Nathorst and Schweitzer collections, reach respectively 9.5, 7.5 and 7.3 cm in width (Fig. 3A-C). The main stem displays in its exposed surface at least three straight and continuous ribs crossing a curved nodal line on which are inserted two truncated secondary axes (Fig. 3A-C). Larger stems are usually straight, rather smooth, and slightly ribbed (Fig. 3A-D). These ribs remain longitudinally uninterrupted throughout the entire length of axes (Fig. 3A-C). Only one or two second order axes were borne per node of the main stem (Fig. 3A, C). These axes are on average 2.8 cm wide and arise obliquely from the first-order axes at an angle of 55° (Fig. 3C). On the specimen S038058, nodes are separated by 14 cm long straight internodes (Fig. 3A). The specimen JE-Sch0067-01 is a 2.25 cm wide second order axis that displays a 3rd order branch scar positioned adaxially to the slightly curved nodal line (Fig. 4A-B). The nodal line appears to be pressed downward due to the slight abaxial extension of the branch base. Above,

the 4.5 mm wide oval shaped branch scar features 6-8 radially arranged ridges surrounding a 1.8 mm wide medullary cavity (pith) a pattern that could be consistent with, though does not conclusively demonstrate, the former presence of a ring of discrete vascular bundles arranged around a pith within an equisetostele (Fig. 4B-C). The asymmetry of the branch scar, combined with the enhanced ridging beneath the medullary cavity, further suggests that the third-order axis emerged at an oblique angle, comparable to the emergence pattern of the second-order axes on the main axis (Fig. 3B).

The most common remains of *P. ursina* are its leaves, generally detached from their original biological insertion on third and fourth order lateral axes. Leaves are only borne on these terminal laterals, on which they are organised in whorls (Fig. 3E-H). Up to four 8 cm long leaves per node were observed (Fig. 3E-G). Nodal diamond-shaped leaf scars are often observed where the leaves used to be attached (Fig. 3F). Leaves are erect, strongly dissected, and characterized by a fimbriate feather-like shape (Fig. 3E-H). On specimen S038054, nodes are separated by 9 cm long straight internodes (Fig. 3G).

Most of these features, including the relatively large width of the main stem, the presence of at least two orders of branches with a nodal insertion, the monopodial branching, the regular whorled phyllotaxy and the Schweitzer's discovery of a several metres long articulate main stem in Bear Island (Fig. 1D), suggest an arborescent habit reminiscent of the tree-like Equisetales of the Carboniferous (Schweitzer, 1967, 2006; Mosbrugger, 1990).

Fertile axes: strobilus, bracts and fertile appendages

The fertile material (Fig. 5) consists of 5 different fertile axes (see Fig. 6 for line drawing and numbering), that are all truncated except axis #4, which remains attached to the main stem node

(Figs 5A, 6B). A fragmentary axis attached to this node (Fig. 5E) may be the base of axis #1 or #2. Its presence also indicates that the node borne at least two strobili, following the architecture of vegetative lower order axes. Preserved fertile appendages (Figs 5-9) were found alongside the uppermost part of axis #1 and scattered along the axes #4 and #5. The additional fertile specimen from the Antevs collection was illustrated in Fig. 10 (Axis #6) and consists of a single axis truncated on both sides but displaying three remaining fertile appendages.

General description of the strobili

The first and second strobili (Axes #1 and #2 on Fig. 6) are truncated both towards the apex and base (Figs 5B, 6A). Axis #1 is 11 cm long, axis #2 measures 8.5 cm. The fertile axes feature slightly curved nodal lines with internodes averaging 11 mm in length. Straight, continuous ribs comparable to those observed in vegetative axes are frequent but not systematically preserved. Axis #1 displays approximately 8 detached sporangial clusters (Figs 5B, 6A), found either above it or between it and axis #2 (Figs 7A-C, 8A & 8C).

Axis #3 is 6.3 cm long, missing its apex, base, and bracts. Its internodes are smooth and ribless (Figs 5A, 6B). Axis #4, the best preserved, includes both apex and base (Figs 5A, 6B). It measures 32 cm, tapering from 8 mm to 2 mm in diameter distally, with internodes averaging 9.3 mm in length. Ribbing is prominent at its base with 2 to 4 ribs separated by furrows (Figs 5E, 6B). At least 8 fertile appendages are present (Figs 5C-D, 6B), including one with a preserved stalk and insertion (6D-G, 7B & 7D).

Axis #5, possibly part of axis #3, is 10.1 cm long and lacks apex, base, and most bracts (Figs 5D, 6B). At least 3 distinct fertile appendages are scattered besides it (Figs 5D, 6B). Among them, the best-preserved fertile appendage displays obovate sporangia arranged in rows (Fig.

7H).

Axis #6 is 7.8 cm long, truncated at both apex and base and displays four attached bracts and three associated sporangial clusters (Fig. 10A-B). Additional torn bracts are scattered along the axis. Internodes, averaging 8.8 mm long, exhibit a rather smooth stem with longitudinal ribs and furrows, and small vascular traces (fertile appendage + bract scars) are observable on the 4th and 5th nodes (Fig. 10B-D). Features displayed by each of the strobilus are summarised in Table 1.

Bracts

Bracts are borne in whorls and are generally distally torn. They bifurcate only once, proximally without any pedicel, with each segment measuring 2 mm wide and 17 mm long, on average and exhibiting a striate lamina with a strong parallel venation (Figs 5C, 7E, 8B). Bracts are reflexed and decurrent, emerging at an oblique angle of 48°. They are slightly erect near the base but curve downward distally, often covering internodes. Fertile axes #2 and #6 bear numerous bracts, while axis #1 displays bracts only proximally (Fig. 5).

Compared to vegetative leaves, bracts tend to widen distally and may develop a wedge-shaped morphology. For example, a bract from node 14 of axis #4 is 11 mm long and displays an entire margin rather than the dentate or fimbriate margins typical of vegetative leaves (Fig. 7D, 8D). The number of bracts per node is difficult to assess, as many may have been removed or torn before fossilization. However, a few bracts were found attached frontally at the middle of nodes (Fig. 10B), and diamond-shaped vascular traces (Fig. 10C-D), similar to those (leaf scars) left by vegetative leaves (Fig. 3F), were observed on the 4th and 5th nodes of axis #6.

Fertile appendages

Axis #1 bears 8 detached sporangial clusters, with three fertile appendages on nodes 11–13 that keep their short stalks (Figs 5B, 6). The second reproductive structure from the bottom of the axis displays the best-preserved stalk measuring 1.5 mm long and 0.7 mm wide (Figs 6A, 7A, 8C). Another example is present in the uppermost part of the specimen, with a fertile appendage with a stalk measuring 1.7 mm in length and 1.1 mm in width (Figs 7C, 8A). On axis #4, another fertile appendage is identified at node 17 with the stalk reaching 1.4 mm in length and 0.8 mm in width (Figs 5C-D, 6B), being seemingly attached to the adaxial leaf surface and supports a receptacle with over 20 densely packed sporangia (Figs 7E, 8B). On the 14^{th} node, there is a 6.4 mm long fertile appendage displaying a wide-obconical receptacle and a long stalk measuring 5 × 0.5 mm (Figs 7D, 8D). The fertile appendage is heavily crushed from the top and its original insertion is on the bract axil. This axillary insertion of the fertile appendage is also suggested by the one that was inserted on the 26^{th} node of the axis #4, showing a 5 mm long elongated stalk (Fig. 7G). At node 19 of axis #4, a particularly large sporangial cluster subtended by a damaged bract highlights differences in preservation states of the fertile appendages. Stalks are completely overlapped and therefore only inferred. Axis #6 bears three sporangial clusters attached with two fertile appendages on nodes 4–5, both retaining their stalks (Fig. 10). The lowermost fertile appendage on the 4^{th} node has a stalk measuring 5.2 × 0.7 mm, though its connection to the bract is not observed (Fig. 10A-B). The second fertile appendage features a fragmentary stalk, up to 32 heavily compressed sporangia, and a subtending bract still attached to the node (Fig. 10C-D).

Most of these reproductive structures are heavily damaged, laterally crushed and sometimes shredded. Fertile appendages along axis #1 have a receptacle on which elongated and obovate-shaped sporangia with almost parallel margins are inserted (Figs 7B-C, 8A). Sporangia are densely packed and inserted radially on the receptacle (Fig. 7B, H). In cases of lateral

compression, only peripheral sporangia are visible, overlapping those beneath. The exact number of sporangia per appendage is difficult to determine due to preservation, but a fertile appendage on axis #4 at node 16 retains up to 33 sporangia compressed from the top and likely organised in concentric circles (Figs 7F, 9A-B), suggesting total counts may exceed 35 per appendage. In the three selected fertile appendages represented in the line drawing (Fig. 8A-B), measurements indicate sporangia average lengths of 2.6, 3.5 and 3.3 mm and average widths of 0.64, 0.72 and 0.67 mm respectively (Figs 7B, 8A-B). Two fertile appendages illustrate the effects of lateral compression, appearing highly elongated and less compact, with one on the 26th node of axis #4 and another on the 6th node of axis #5 (Fig. 7G-H). By contrast, appendages with minimal compression preserve densely packed sporangia inserted on a tentatively interpreted as dome-shaped or circular receptacle, such as one above axis #1 and another near the 17th node of axis #4 (Figs 7C, 8A-B).

In situ spores

In situ spores are cavate, trilete (Fig. 11A), and possess an exoexine (= perispore) that extends equatorially, forming an equatorial zona (Fig. 11A-F). The amb is circular to sub-circular. The intexine forms a distinct subcircular to triangular inner body, with straight laesurae restricted to the intexine. The central area is typically opaque, often obscuring the trilete scar in proximal view (Fig. 11A, D-E). The spores of *P. ursina* exhibit minimal variation in size and shape, with a total diameter of 176.5 μm and an average central area diameter of 74 μm. Among all examined thin sections, these spores are the largest observed within the *sporae dispersae*. Notably, *P. ursina* spores feature radially arranged ribs or folds within the extended exoexine, radiating from the intexine to the periphery. The spore species that best corresponds to this description is *Auroraspora solisorta* Hoffmeister, Staplin & Malloy, 1955.

Phylogeny

Phylogenetic relationships in the maximum parsimony analysis

Our maximum-parsimony analyses using implied weighting (k = 3, 6, 9, and 12), based on the full character and taxon sampling, yielded 6 most-parsimonious (MP) trees for k = 6, 9, and 12 (total fit = 6.840, 4.944, and 3.874, respectively), and 12 MP trees for k = 3 (total fit = 11.171). The strict consensus trees obtained with k = 6, 9, and 12 are highly similar and recover the Equisetales and the Bowmanitaceae as monophyletic and presenting some polytomies (Fig. 12). The strict consensus tree obtained with k = 3 is also broadly comparable but remains less resolved due to an additional polytomy among cladoxylopsids (Fig. S1). The equal-weights parsimony analysis, using the same search strategy, resulted in 60 MP trees (TL = 140; CI = 0.614; RI = 0.805). Its strict consensus is markedly less resolved than any of the implied-weighted trees and collapses most stem-sphenopsid relationships—including *Rinistachya*, *Eviostachya*, *Hamatophyton*, the Bowmanitaceae, the *Lilpopia–Peltastrobus* clade, and the Equisetales—into a broad polytomy (Fig. S2). The polytomy of Equisetales includes Angaran-Gondwanan (A.G.) sphenopsid species: *Paracalamitina striata* (Angara) and *Cruciaetheca patagonica* (Gondwana), and two distinct clades: the Calamitaceae and Equisetaceae + *Neocalamites*; and the polytomy of the Bowmanitaceae is composed of *B. moorei*, *B. dawsoni*, *Leeites oblongifolis* and a small clade of two *Bowmanites* species (*B. myriophyllus* and *B. priveticensis*). The Bowmanitaceae clade is defined by two synapomorphies: the presence of fertile appendages partially fused with bracts and two sporangia per fertile appendage (Char. 31, 36 - Fig. 13). Notably, *Bowmanites* species are also marked by loosely constructed strobili, shielded fertile appendages, and vascularized sporangial shields (Figs 12, S1 and S2). The Bowmanitaceae are recovered sister to the *Peltastrobus-Lilpopia* clade, which is defined by two

synapomorphies: the polytomous division of the fertile appendage and the presence of fertile and foliar appendages diverging on alternate radii of the same node (Char. 29, 45 - Fig. 13). Within this small clade, *Peltastrobus reedae* features intricate vascular structures, whereas *Lilpopia raciborskii* is distinguished by its elongated wedge-shaped leaves and compact strobili. These two clades (Bowmanitaceae + *Peltastrobus-Lilpopia* clade) compose the monophyletic group of the Sphenophyllales, resolved sister to the Equisetales and defined on three homologies: the presence of wedge-shaped leaves, a prominent heterophylly and the monolete aperture of spores (Char. 5, 7, 56 – Fig. 13). Within the equisetalean clade, the polytomy that includes the A.G. species, the Calamitaceae (*Palaeostachya guanglongii*, *Calamostachys americana* + *Calamostachys binneyana*) and *Neocalamites* sp. + Equisetaceae (*Equisetites arenaceus* + *Equisetum* spp. including both extinct and living species) is recovered sister to the Archaeocalamitaceae (*Protocalamostachys arranensis*). Together, they form an equisetalean clade, in accordance with the parsimony based phylogenetic analysis of Elgorriaga *et al.*, (2018), that is defined by the following five synapomorphies: the restrictive number of branching orders (one to two), the presence of fertile appendages inserted on internodes, a shield development for the entire fertile appendage, the absence of bracts and the presence of whorls of vegetative units regularly alternating with whorls of fertile appendages at successive nodes (Char. 18, 31, 33, 35, 46 – Fig. 13).

Cheirostrobus and *Pseudobornia* fall within an expanded equisetalean lineage in our analyses, they are thus also considered as stem-group Equisetales. *Pseudobornia ursina* exhibits traits such as an arborescent habit, longitudinally ribbed stems and a hollow stem core (medullary canal), suggesting the development of an equisetostele (Char. 19 and 21 – Fig. 13). These features support its interpretation as an early representative of the equisetalean lineage, positioned as sister to the remaining Equisetales. Our parsimony-based analyses likewise recovered *Cheirostrobus pettycurensis* as sister to the rest of the clade, and the total group

Equisetales is now defined by three characters: the fertile appendage insertion in the bract axil, the elongation of the sporangium and its insertion mode as sessile (Char. 31, 39, 40 – Fig. 13). The inclusion of *Cheirostrobus* within this evolutionary lineage is consistent with hypotheses proposed by Neregato and Hilton (2019), emphasizing its relationship to the Calamitaceae clade.

Sphenophyllales and Equisetales are also recovered as sister groups, forming a clade defined by four synapomorphies: the presence of xylem rays and secondary xylem, a shield development for individual stalks and the presence of bracts (Char. 24, 25, 33, 35 – Fig. 13), the latter character being also observed outside of the group, with *Rinistachya hilleri* (Fig. 16A). Our parsimony-based phylogenies align thus with prior studies regarding the placement of Equisetales and Sphenophyllales as sister groups within Sphenopsida (Boureau, 1964; Elgorriaga *et al.*, 2018).

Late Devonian taxa (*Rinistachya hilleri*, *Eviostachya hoegii*, and *Hamatophyton verticillatum*) are resolved as stem-group sphenophytes, forming a paraphyletic grade basal to the sphenopsid clade (Figs 12, S1). *Hamatophyton*, recovered sister to the rest of the sphenopsid clade (Equisetales + Sphenophyllales), shares with them an undivided fertile appendage and the lack of paired sporangia (Char. 29, 37 – Fig. 13). *Eviostachya* is recovered sister to the rest of the above mentioned sphenopsid clades (*Hamatophyton*, Sphenophyllales + Equisetales), and the common character is the presence of a ribbed stem (Char. 2 – Fig. 13).

Total group Sphenopsida includes finally *Rinistachya hilleri*, being resolved sister to a clade comprising all other sphenophytes. Three characters define the clade Sphenopsida, including *Rinistachya*: the presence of leaves (planate and webbed laminar organs) and the trichotomous division of fertile appendages with two successive branching (Char. 5, 29, 30 – Fig. 13).

Cladoxylopsids are resolved as a paraphyletic grade, subdivided into three distinct clades: Cladoxylales, Pseudosporochnales and Iridopteridales. *Denglongia hubeiensis* and *Panxia*

gabata constitute a cladoxylopsid clade corresponding to the Cladoxylales, which is supported by five synapomorphies: the presence of planate vegetative appendages, the alternate-opposite taxis of homologous ultimate appendages, two branching orders, erect sporangia and the absence of paired sporangia (Char. 4, 12, 18, 37, 38 – Fig. 13). This monophyletic group is recovered sister to a clade comprising the Pseudosporochnales and the clade that includes the Iridopteridales and Sphenopsida. In our parsimony-based analyses with equal and implied weights, *Pseudosporochnus nodosus* and *Calamophyton primaevum* are resolved within a clade: the Pseudosporochnales. This group is featured by two main synapomorphies: an arborescent habit and the presence of digitate branching (Char. 1, 14 – Fig. 13). The Iridopteridales, recovered as monophyletic, are composed of *Ibyka*/*Anapaulia* and *Compsocradus laevigatus.* This clade is resolved as the sister group of Sphenopsida, forming thus a single monophyletic group (Iridopteridales + Sphenopsida) defined by four synapomorphies: the presence of whorled or pseudo-whorled arrangement of vegetative appendages, branching consistently associated with nodes, an actinostele-type of protostele in aerial vegetative stems, and the presence of whorled fertile appendages (Char. 12, 15, 19, 44 – Fig. 13). Time-scaled phylogenies suggest Iridopteridales diversified rapidly during the Middle Devonian, and sphenophytes might have emerged from their cladoxylopsid hypothetical common ancestor as early as the middle Eifelian. A second radiation occurred in the Famennian (Late Devonian), producing the distinct clades of Sphenophyllales. and the Equisetales comprising *Pseudobornia* and *Cheirostrobus*. (Figs 12, S1 and S2).

Bayesian vs. parsimony analyses

Bayesian inference (Fig. 14) reveals differences compared to parsimony-based analyses (Figs 12, S1 and S2). In the Bayesian topology, Calamitaceae and the A.G. species are paraphyletic, forming successive grades leading to crown Equisetaceae (*Equisetum* spp.).

Sphenophyllales remains monophyletic, with *Peltastrobus* and *Lilpopia* forming a clade sister to the Bowmanitaceae. The latter is fully resolved and includes two distinct sister monophyletic groups: (*B. myriophyllus* + *B. priveticensis*) and (*B. moorei* + *Leeites oblongifolis, B. dawsoni*). *Cheirostrobus pettycurensis* and *Pseudobornia ursina* show differing placements compared to parsimony: the former is assigned to the Sphenophyllales, recovered sister to the rest of the sphenophyllalean clade, while the latter is positioned prior to the divergence of Sphenophyllales and Equisetales, being therefore resolved sister to a clade comprising both. With the exclusion of *P. ursina* from the Equisetales in the topology resulting from the Bayesian inference, the divergence between Equisetales and Sphenophyllales occurred in the early Tournaisian (Mississippian) rather than during the Famennian (Late Devonian) (Fig. 14). Moreover, the results of the Bayesian inference also point out differing positions of the stem sphenopsids: *Rinistachya, Eviostachya* and *Hamatophyton.* Instead of *Rinistachya*, a clade composed of *Hamatophyton* and *Eviostachya* is recovered sister to all other sphenophytes in the resulting maximum clade credibility tree (Fig. 14).

DISCUSSION

Reconstruction

The strobilus morphology of *P. ursina* is reconstructed based on the most complete axis (#4), which is still attached to the main monopodial trunk or a first order branch (Fig. 15A). Strobili were 30 cm long and loosely constructed, bearing at each node tentatively three to four whorled, bisected laminar bracts that subtended the fertile appendages. Bracts were apparently more upward oriented distally and drooped downward proximally. The number of bracts per whorl is inferred from vascular traces, a frontally inserted bract at the 8th node (Fig. 8A–B), and from

the number of leaves per whorl observed on vegetative axes. The internodal length diminishes upward, making the strobilus looks more compact distally.

A reconstruction of the fertile unit (bract + fertile appendage) is proposed herein (Fig. 15B). Based on the various preserved fertile appendages and associated bracts, the strobilus likely had erected sporangia-bearing receptacles borne on a stalk and obliquely inserted on the bract axil. Fertile appendages bear at least 30 to 40 elongated sporangia, which were erect and probably inserted in concentric circles (Fig. 9A-B) on a wide-obconical receptacle. After careful observations of the sporangia and preserved appendages, no short stalks were seen linking the sporangium to the rest of the fertile appendages. Therefore, sporangia are interpreted as sessile, being directly inserted on the receptacle. At first glance, bracts appear fimbriate and closely resemble the morphology of vegetative leaves. However, only one division occurs in the bracts whereas the vegetative leaves underwent successions of leaf divisions. Additionally, some evidence suggests an entire margin and a heavily striated lamina, which are not seen in the sterile leaves.

Our reconstruction (Fig. 15) stands in between the previous propositions of S. Leclercq and H.J. Schweitzer, although it is more aligned with the former (Gothan and Weyland, 1973; Schweitzer, 2006). We indeed favour loose sporangial cluster borne adaxially in the axil of a bisected bract with entire margins, as did S. Leclercq (Gothan and Weyland, 1973), rather than the *Lilpopia*-like morphology of globose sporangial clusters subtended by a fimbriate bract from H.J. Schweitzer (Schweitzer, 2006).

Nevertheless, we propose fertile appendages that are more compact than in Leclercq's reconstruction (Gothan and Weyland, 1973). The "globular-shaped sporangia" with polygonal margins proposed by Schweitzer (2006) resulted from the literal interpretation of a fertile appendage that was compressed from the top (Figs 7F, 9A-B), while the loosely constructed fertile appendages protected by an extended "cup-shaped receptacle" from S. Leclercq (Gothan and Weyland, 1973) likely came from the observation of heavily crushed elements with a lateral

compression, which tends to give an oversized representation of the fertile part bearing loosely packed sporangia (Fig. 7D).

Comparisons

In the Late Devonian, several stem-group sphenophytes can be compared to the fertile whorls of *Pseudobornia ursina*. Among them, *Hamatophyton verticillatum* Gu & Zhi (1974) from the Famennian and early Mississippian of South China is currently one of the best-known Devonian sphenophytes. Despite being contemporaneous with *Pseudobornia*, *Hamatophyton* differs markedly. Based on the most complete specimens (Wang & Guo, 2009), *Hamatophyton* is characterised by simple fertile whorls, each bearing a single recurved spiny sporangium atop a 2.5 mm stalk (Wang *et al*., 2006; Wang & Guo, 2009). These whorls are directly inserted on the node and lack a prominent subtending bract, a feature present in most non-equisetalean sphenophytes. In contrast, *Pseudobornia* has nodal whorls of bifurcated bracts with large, erect fertile appendages inserted axillary. Each appendage bears at least 30 erect sporangia disposed terminally on a wide-obconical receptacle facing away from the fertile axis. Despite both genera exhibiting determinate growth leading to a loosely constructed strobilus, *Hamatophyton* possesses the simplest fertile structures among sphenopsids. It lacks complex appendage subdivisions, shields, or associated bracts, making its fertile organs fundamentally different from those of *Pseudobornia ursina*.

Rinistachya hilleri Prestianni & Gess (2019), from the Famennian of the Waterloo Farm Lagerstätte (South Africa), is a stem sphenopsid sharing key traits with *Pseudobornia.* Both exhibit axillary insertion of the fertile appendage and bisected bracts (Fig. 16A). Like *Pseudobornia, R. hilleri* bears multiple sporangia associated with a bract, and their insertion in the leaf axil points to a basal fusion of fertile appendages with the bracts, a feature suggestive of affinities with the Sphenophyllales. Despite this morphological similarity, it is recovered in

our analyses as a stem-group Sphenopsida. Bracts are smaller and simpler than vegetative leaves, which in both taxa are long (~8 cm) and regularly divided. However, *Pseudobornia* shows more pronounced heterophylly, with strongly veined, non-fimbriate bracts. Fertile appendages of *R. hilleri* feature two successive trichotomies with paired sporangia (Fig. 16A), forming a loose, complex structure distinct from the undivided stalked appendages of *Pseudobornia.* Additionally, *R. hilleri* has a straight, smooth-stemmed strobilus that is more loosely constructed.

Eviostachya hoegi Stockmans (1948), from the Famennian of Belgium and China (Leclercq, 1957; Wang, 1993), also has a complex fertile appendage with spines, bearing three sporangia per sub-stalk and totalling 27 sporangia (Fig. 16B). Its structure, with two successive trichotomies, resembles *Rinistachya* in organ arrangement and sporangia count but is more compact, forming a denser strobilus than both *Rinistachya* and *Pseudobornia. Eviostachya* is distinguished both from *Rinistachya* and *Pseudobornia* by the total absence of a bract and thus by the perpendicular insertion of the fertile appendage on the fertile axis, which reminds the morphological patterns of the equisetalean fertile whorls.

Peltastrobus reedae Baxter (1950) from the Pennsylvanian of the U.S. is a loosely constructed strobilus with fertile whorls composed of three vegetative leaves alternating with three fertile units. Each unit consists of five peltate sporangium-bearing stalks subtended by a forked bract (Fig. 17A). The fertile appendages are both perpendicularly inserted to the fertile axis and axillary to the bract, with their bases fused. Proximally, they undergo polytomous division into five stalks per bract (Leisman & Graves, 1964; Baxter, 1972), each bearing over 40 sporangia, almost entirely covered by a thickened cell layer forming a peltate shield. While *Peltastrobus* and *Pseudobornia* share a loosely constructed strobilus with fertile whorls of appendages subtended by a bract and bearing numerous elongated sporangia, their similarities do not extend further. *Pseudobornia* lacks the complex appendage organisation, vegetative-

reproductive alternation within nodes, and peltate stalks characteristic of *Peltastrobus.*

Lilpopia raciborskii (Conert & Schaarschmidt) Lipiarski (1972a), known from the Carboniferous and Permian of Poland, Germany (Kerp, 1984), and more recently from fragmentary remains from Argentina putatively assigned to this genus (Cariglino, 2013), belongs to the Sphenophyllales. It features lateral second-order axes with intercalated fertile segments between vegetative ones, indicating indeterminate growth and the absence of a true strobilus. Its fertile segments consist of whorls of three massive, strobilus-like structures, considered as fertile appendages, alternating with three wedge-shaped vegetative leaves (Kerp, 1984) (Fig. 17B). These compact, cone-like structures, interpreted as peltate stalks, fit together to form a stalked reproductive body (Lipiarski, 1971, 1972a; Kerp, 1984). *Lilpopia* differs sharply from *Pseudobornia* in its alternating vegetative and fertile appendages within the same node, reproductive structure organisation, presence of a thickened cell layer acting as a shield, and absence of a bract.

Pseudobornia ursina can also be compared with the enigmatic sphenopsid species: *Cheirostrobus pettycurensis* (D. H. Scott) Neregato and Hilton (2019), which stands as a strobilus made of whorls of three-lobed bracts of a cuneate shape. An elongated fertile appendage is inserted on each bract axil, bearing four elongated sporangia, two adaxially and two abaxially. A leafy fertile appendage apex seems to play the role of a shield, and it partly covers the four sporangia attachments. *Pseudobornia* shares with *Cheirostrobus* the determinate growth allowing the development of a strobilus and the axillary insertion of a unique fertile appendage to the bract axil. Whereas they differ in the structure of the fertile appendage, the orientation, number and insertion of sporangia and the morphology of the bract. Furthermore, isospores of *C. pettycurensis* are circular, trilete and lack a perispore (=exoexine). While spores of *P. ursina* are trilete and cavate with an extensive development of their perispores.

Carboniferous Bowmanitaceae (= Sphenophyllaceae) are well-represented in the fossil record, including *Bowmanites* and its allies (e.g. *Sphenostrobus, Leeites,* and *Litostrobus*). *Bowmanites*, a morphogenus often linked to *Sphenophyllum*, exhibits diverse strobilar morphologies, particularly in fertile appendage insertion, sporangia count, and overall structure. Some suggest it may not represent a single natural group (Good, 1978). *Bowmanites dawsoni* (Williamson) Weiss (1884) and *B. moorei* Mamay (1959) have cuneate bracts with a basal lateral fusion, supporting one or two simple fertile appendages that each bear a single recurved sporangium near the bract axil. Their strobili are more compact than in other Sphenophyllales. Similarly, *Sphenostrobus thompsonii* Levittan & Barghoorn (1948) and *Bowmanites angustifolius* (Germar) Hoskins & Cross (1934) exhibit a fused fertile appendage-bract structure, though their sporangia are erect (Good, 1978). In contrast, Pennsylvanian species *B. myriophyllus* and *B. priveticensis* (Libertín *et al*., 2014) bear four to five recurved sporangia per appendage but lack laterally fused bracts, resulting in a more linear aspect. Overall, *Bowmanites* and *P. ursina* share bract-fertile appendage fusion, adaxial insertion, occasional dichotomous division of the bract, and determinate strobilus growth. However, *Pseudobornia* differs in its reduced heterophylly, lack of terminal hooks, and erect, shield-free sporangia exceeding 35 in number. Additionally, bracts and fertile appendages are less fused in *P. ursina*, with sporangia arranged on a wide-obconical receptacle.

Although their strobili differ, *Pseudobornia* closely resembles *Calamites* and *Archaeocalamites* (Brongniart) Stur in vegetative morphology, sharing a monopodial trunk and lateral branches at nodes. Moreover, the available adpressions have been interpreted as suggesting an equisetostele-like organization (Fig. 4) (Schweitzer, 1967, 2006), although this inference remains tentative given the absence of direct evidence from anatomically preserved axes. Regarding the fertile axes, Equisetales are characterised by fertile phytomers producing fertile appendage whorls along internodes. Thus, equisetalean fertile appendages are

perpendicularly inserted to the cone axis and are never fused to an eventual bract. Equisetalean fertile axes often exhibit a determinacy of apical growth allowing the development of compact strobili as in *Peltotheca* (Archaeocalamitaceae), *Calamostachys* (Calamitaceae) or even the crown-group *Equisetum* (Equisetaceae), while some other equisetalean sphenophytes had an indeterminate growth like *Cruciaetheca* (Cúneo and Escapa, 2006; Tomescu *et al.*, 2017). Calamitacean strobili (e.g. *Calamostachys, Palaeostachya, Mazostachys, Pendulostachys*) feature alternating whorls of fertile appendages and sterile bracts (Arnold, 1958) whereas Archaeocalamitaceae bear multiple fertile whorls per internode and Equisetaceae display a strobilus constituted with a single fertile phytomer lacking node-internode differentiation, that bears multiple fertile whorls (Tomescu *et al.*, 2017). *Pseudobornia*, conversely, has a loosely constructed strobilus of fertile nodes and sterile internodes, opposite to Equisetales. Furthermore, equisetalean sporangiophores bear a shield or peltate tip, as in *Peltastrobus reedae* and *Lilpopia raciborskii*, while *P. ursina* entirely lacks these features, possessing axillary fertile appendages with terminally inserted erect sporangia. This fundamental distinction highlights major differences between the fertile structures of *Pseudobornia* and the rest of Equisetales.

The systematic position of *Pseudobornia ursina*

The early evolution of sphenophytes is a subject of significant interest in paleobotany due to their unique morphology and uncertain relationships with other monilophytes. This clade, which dates back to the Late Devonian, has sparked decades of research to elucidate the evolutionary innovations that led to the prominence of sphenopsids during the Carboniferous and beyond (Boureau, 1964; Skog and Banks, 1973; Stein *et al.*, 1984; Rothwell, 1999; Wang and Guo, 2009; Tomescu *et al*., 2017; Elgorriaga *et al*., 2018). *Pseudobornia ursina* is a key taxon to understand this radiation, being one of the oldest known sphenophytes and displaying

an array of morphological vegetative and fertile features that were historically interpreted either as sphenophyllalean or equisetalean (Boureau, 1964; Schweitzer, 2006). Nevertheless, *Pseudobornia* has been so far neglected in the uncovering of the evolutionary history of Sphenopsida and its systematic position remained uncertain.

Pseudobornia bears an unusual mosaic of characters among sphenophytes, which lead to the erection a new order (i.e. Pseudoborniales) for its accommodation (Nathorst 1902: Schweitzer 1967). Boureau (1964) noted that *Pseudobornia ursina* shares a key vegetative trait with early "sphenophyllales", namely laciniate leaves (Fig. 18). Late Devonian sphenophytes generally had simpler, webbed appendages (Deng *et al*., 2016), though some, like *Sphenophyllum lungtanense* and *Xihuphyllum megalofolium*, displayed more advanced cuneate leaves (Huang *et al.,* 2017, 2022) (Fig. 18). Despite its laciniate leaves suggesting a plesiomorphic state, *P. ursina* exhibits fimbriate margin and a more developed lamina emphasising a complexification of the leaf morphology and may represent a more derived structural adaptation. However, unlike the diminutive forms typical of Sphenophyllales, its arborescent habit and hollow stems (inferred from branch scars comparable to those of *Calamites cruciatus*), contrasts sharply with the protostelic anatomy of Sphenophyllales, therefore more closely resembling Equisetales in that regard.

Pseudobornia ursina exhibits several autapomorphic features in its fertile parts. Indeed, they stand as sessile, erect (char. 37) and elongate sporangia borne at the tip of a stalk that is widening distally to form a wide-obconical receptacle (Fig. 15B). The compact aspect of the fertile appendage combined with the large number of sporangia borne on each receptacle contrast sharply with the looser fertile appendages in *Rinistachya* and *Eviostachya* (Leclercq, 1957; Prestianni & Gess, 2019) in which several trichotomous divisions can be identified combined with substalks bearing recurved sporangia. The erect aspect of the sporangia of *Pseudobornia*

and their insertion on the receptacle seems to be the reverse of the insertion mode of sporangia in Equisetales, standing as an upside-down receptacle bearing sporangia on the abaxial surface and covering them by forming a peltate shield (= sporangiophore). Moreover, the axillary insertion of the fertile appendage with its bract can be compared to those of *Rinistachya hilleri* and to a lesser degree *Cheirostrobus pettycurensis*, *Peltastrobus reedae*, *Hexaphyllostrobus kostorhysii* (D'Antonio *et al.*, 2024) and even some equisetalean sphenopsids like *Palaeostachya* and *Weissistachys*, considering the possibility that bract and fertile appendage departures in *Pseudobornia* could also be distinct. The association with a bract and the morphology of the fertile appendages belonging to *Pseudobornia* rather suggests an affinity with early stem sphenopsids historically assigned to Sphenophyllales. *Pseudobornia* is thus characterised by a mosaic of fertile traits frequently seen in sphenophyllalean mixed with vegetative structures and habit typical of equisetaleans.

In the phylogenetic analyses using parsimony, *Pseudobornia* is recovered as a stem Equisetales despite having very distinctive fertile appendages (Figs 12, S1 and S2). The morphology of the laciniate vegetative leaves and fertile appendages associated with a bract are therefore interpreted as plesiomorphic characters that emerged before the appearance of Sphenophyllales and Equisetales, with the stem sphenopsids. On the other hand, the siphonostelic stem (= equisetostele) and the arborescent habit are considered more derived and thus apomorphic, compared to the vegetative characters of stem sphenopsids and the fertile traits of *Pseudobornia*. We showed that *Pseudobornia* was also more closely related to the Archaeocalamitaceae. Hence, according to our parsimony-based phylogenies, *Pseudobornia* is considered as an early member of the Equisetales, implying the deletion of the Pseudobornialean order.

Nevertheless, another evolutionary scenario is drawn by the Bayesian inference of phylogeny

in which *Pseudobornia* is placed slightly more stemward, prior to the divergence of Sphenophyllales and Equisetales (Fig. 14), within a grade that includes *Eviostachya*, *Hamatophyton* and *Rinistachya.* This grade is therefore composed of stem sphenopsids, that are not yet differentiated between the two major clades of sphenophytes (Sphenophyllales and Equisetales). Thus, according to the Bayesian inference of phylogeny, *Pseudobornia* was a stem sphenophyte with equisetalean vegetative traits (Fig. 14). However, Bayesian "tip-dated" analyses with morphological clock (Mk + FBD) can be pulled towards groupings that maximize stratigraphic concordance, sometimes at the expense of characters (Luo *et al*., 2020; King, 2021). Time calibration that heavily influenced the Bayesian analysis, possibly prevented the formation of some clades that are recovered in the parsimony-based phylogeny (e.g. Calamitaceae), if not enough synapomorphies were computed to counterbalance the time influence. Therefore, it could explain the differences observed in tree topologies in between parsimony and Bayesian based analyses. *Pseudobornia*, a Late Devonian taxon, was positioned within the stem sphenopsids, sister to the Equisetales and Sphenophyllales, due to the FBD model favouring placements that follow consistently the stratigraphy. This time influence also explains the gradual evolution of Equisetales without any cladogenesis. Therefore, we have favoured results obtained from parsimony-based analyses over Bayesian inferences because they are more reliable, relying on character-based relationships rather than stratigraphy.

Origin and evolution of vegetative and fertile traits of sphenopsids

Fertile appendages, traditionally referred to as "sporangiophores" within Sphenopsida, exhibit remarkable structural diversity throughout the late Paleozoic (Arnold, 1958; Boureau, 1964; Baxter, 1972; Good, 1978; Kerp, 1984; D'Antonio *et al.*, 2024). Stein *et al*. (1984) were among the first to apply parsimony-based phylogenetics to both vegetative and fertile structures of stem

monilophytes, proposing and testing alternative phylogenetic hypotheses for the origin of the sphenopsids. Based on three different characters related to the primary xylem configuration (1), arrangement of leaves or homologous laterals (2) and the organisation of fertile appendages (3), three hypotheses consistent with stratigraphy stood out. One of these hypotheses in which no parallelism or reversal was assumed for the organisation of fertile appendages, suggesting that Sphenopsida derived from the "Hyeniales" (*Calamophyton* + *Hyenia*), as did Skog & Banks (1973). *Ibyka* was also considered as an intermediate taxon between Trimerophytes and the cladoxylopsids in all three hypotheses, being formerly attributed to its own order: Ibykales after Skog and Banks (1973). Our phylogenetic analyses recovered Iridopteridales (including *Ibyka*) within Cladoxylopsida *sensu* Berry and Stein (2000), sister to the total-group Sphenopsida (Figs 12, 14, S1, S2), as did Berry *et al*. (2022). The whorled arrangement of axes, although sometimes incomplete, represents a key morphological link between Sphenopsida and their closest relatives (Iridopteridales), contrasting with the helical arrangements seen in Cladoxylopsida (e.g., *Metacladophyton* and *Anapaulia*, which exhibit whorled lower-order axes but helical or opposite higher-order axes; Berry and Edwards, 1996; Wang and Geng, 1997). Additionally, planate but unwebbed lateral organs in these taxa are considered precursors to modern monilophyte leaves. Earlier studies proposed multiple, polyphyletic origins for sphenophytes. For instance, one of the three phylogenetic hypotheses of Steins *et al*. (1984) suggested that Sphenophyllales could derive from the Iridopteridales, while Equisetales originated from "Hyeniales" when no reversal or parallelism was considered for xylem configuration. However, the mosaic of characters in *Pseudobornia ursina* supports the hypothesis that Equisetales originated within stem sphenopsids. Our analyses reinforce the monophyly of sphenophytes, being resolved as the direct sister group to Iridopteridales, which implies that they both evolved independently from a hypothetical common cladoxylopsid ancestor, probably dating back to the Middle Devonian (Figs 12-14, S1, S2).

Before the emergence of megaphylls, fertile appendages were already well-developed in Devonian plants, from trimerophytes to cladoxylopsids (Stein *et al.*, 1984). In Cladoxylopsida, these structures were helically inserted on the axis, undergoing multiple dichotomous divisions, with terminal stalks bearing paired elliptical sporangia. This organisation evolved into more complex patterns, such as the recurved sporangia-bearing stalks of *Calamophyton* (Leclercq, 1969) and the loosely whorled arrangements observed in Iridopteridales (Skog & Banks, 1973; Berry & Edwards, 1996b; Berry & Stein, 2000; Wang, 2008; Fu *et al*., 2011; Berry *et al*., 2022).

A significant evolutionary transition occurred in the Late Devonian with the first appearance of laminate vegetative and fertile leaves (bracts). Stem sphenopsids such as *Hamatophyton* and *Eviostachya* lacked associated bracts, whereas *Rinistachya* and the equisetalean *Pseudobornia* developed fertile bracts subtending sporangia-bearing stalks (Leclercq, 1957; Li *et al.*, 1995; Wang *et al*., 2006; Wang & Guo, 2009; Prestianni & Gess, 2019). In our phylogenetic framework, *Rinistachya hilleri* represents the sister taxon to all remaining sphenophytes, featuring multiple trichotomous divisions of fertile appendages, paired sporangia, and loosely recurved stalks—traits reminiscent of plesiomorphic cladoxylopsid structures (Fig. 13). Despite lacking bracts, *Eviostachya* shares a comparable division pattern with *Rinistachya*, justifying their placement as sister to all remaining sphenophytes. The loss of bracts in *Eviostachya* and *Hamatophyton* was followed by their reappearance in Sphenophyllales and stem Equisetales (*Pseudobornia* + *Cheirostrobus*), only to be lost again in Archaeocalamitaceae (Equisetales). Our parsimony-based phylogenies also recovered *Cheirostrobus* as the sister taxon to all remaining Equisetales due to shared features with some Calamitaceae (e.g. *Palaeostachya* Weiss and *Weissistachys* Rothwell and Taylor) thus supporting both part of the systematic conclusion of Neregato and Hilton (2019) and a closer kinship between *Pseudobornia* and *Cheirostrobus* as suggested by Scott (in Gothan and Weyland, 1973).

Bayesian phylogenetic inference (Fig. 14) suggests that fertile bracts emerged in *Rinistachya* and *Pseudobornia* alongside the axillary insertion of fertile appendages. Bracts persisted in Sphenophyllales (e.g. *Cheirostrobus*, *Lilpopia* + *Peltastrobus*, and Bowmanitaceae), with Bowmanitaceae exhibiting a synapomorphic partial fusion of fertile appendages with their bracts. In contrast, equisetalean evolution was marked by the loss of bracts and the presence of fertile appendage whorls on internodes, leading to the compact strobili of archaeocalamitaceans. This scenario implies that the peltate shields of some Sphenophyllales (e.g. *Peltastrobus* & *Lilpopia*) evolved convergently with those of Equisetales. Furthermore, *Calamites* (*Calamostachys*) appears to conserve some plesiomorphic features compared to other Equisetales, retaining a single fertile appendage whorl per phytomer and a resurgence of nodal bracts (Arnold, 1958; Boureau, 1964). It may be in fact, another by-gone evolutionary pathway that derived from Archaeocalamitaceae, with a reduction in whorl number per fertile phytomer and the reappearance of nodal whorl of bracts (vegetative bracts), characterising the calamitacean lineage within Equisetales. Among late Paleozoic Sphenophyllales, fertile structures seemingly followed two divergent evolutionary pathways. One involved increasing complexity, with polytomously divided stalks and peltate shields, as seen in *Peltastrobus* (Baxter, 1972) and *Lilpopia* (Kerp, 1984). In contrast, those of bowmanitaceans underwent simplification, with reduced fertile structures (Boureau, 1964; Good, 1978; Taylor et al., 2009). Overall, Bayesian and Parsimony based phylogenies yielded almost similar topologies, with the Bayesian maximum clade credibility tree turning out to be better resolved than our parsimony-based phylogenies. The latter represents a possible alternative, worth to be considered and further discussed. Bayesian inferences recovered more consistent placements of taxon with respect to stratigraphy (e.g. the sphenophyllalean affinity of *Cheirostrobus*) and resolved *Pseudobornia,* as a stem sphenopsid sister to both Equisetales and Sphenophyllales, which is also relevant, considering its mosaic of characters. With a clade composed of *Hamatophyton*

and *Eviostachya,* sister to the rest of the sphenopsids, this scenario suggests both that the determinate growth of the fertile axis is a synapomorphy of Sphenopsida and that bracts emerged only once, with *Rinistachya*, rather than two times in the parsimony. However, when considering the xylem configuration of sphenopsids, it seems rather unlikely that an Equisetostele evolved in the typical triangular protostele found in the Sphenophyllales. Bayesian inferences also failed to resolve the equisetalean clades (e.g. Calamitaceae, A.G. clade and Equisetaceae), recovering instead Equisetales as an anagenetic sequence. Thus, these results point out that the characters used likely did not provide enough signal to support the internal clades and that our Bayesian evolutionary model (morphological clock + FBD) may therefore tend to arrange taxa sequentially in time (from fossil 'ancestors' → 'descendants') rather than forming distinct clades. As a consequence, evolutionary scenarios interpreted from our parsimony-based analyses are preferred to those derived from Bayesian inferences.

Our parsimony-based phylogenetic hypotheses (Figs 12–13, S1) indicate that plesiomorphic traits of sphenophyte fertile appendages include: the presence of paired elliptical sporangia (Chars. 37 & 39), and loosely structured strobili (Char. 28) with fertile appendages undergoing successive dichotomous or trichotomous divisions (Chars. 29 & 30). These traits were inherited from Late Devonian stem sphenophytes, marking a pivotal phase in the evolution of this long-lived monilophyte lineage. The loose, divided fertile appendages of early sphenophytes, reminiscent of Iridopteridales, became more condensed in *Rinistachya*, *Eviostachya* and *Hamatophyton*. Bracts likely arose multiple times, providing structural support for large fertile units. Meanwhile, early Equisetales (*Archaeocalamites*) drastically modified their reproductive appendage insertion patterns relative to *Pseudobornia*. Sphenophyllales largely retained plesiomorphic bract-dominated reproductive structures, particularly in Bowmanitaceae. However, evolutionary convergence between the *Peltastrobus-Lilpopia* lineage and Equisetales suggests similar functional pressures shaped their Pennsylvanian

diversification (Lipiarski, 1971, 1972a; Kerp, 1984).

CONCLUSIONS

Pseudobornia ursina, an arborescent sphenopsid uncovered in the Late Devonian deposits of Bear Island, is of prevalent importance to understand the early evolution of Sphenopsida. Fertile axes of *Pseudobornia* were herein re-described, displaying morphological characters considered as plesiomorphic with respect to other equisetalean sphenophytes. These characters are: elongated and erect sporangia borne on the widen tip of a single stalk, forming an obconical receptacle and an axillary insertion involving a bisected bract with entire margins. *In-situ* spores morphologically similar to *Auroraspora solisorta* were also described for the first time. Parsimony-based phylogenies, using a newly compiled dataset of characters, support the position of *Pseudobornia* within Equisetales, being thus recovered as a stem Equisetales, which would make it the oldest known representative of this enduring lineage. Phylogenetic analyses emphasise an evolutionary scenario in which loosely organised, whorled fertile appendages of stem sphenophytes, derived from a cladoxylopsid ancestor common with Iridopteridales, gradually became more condensed and axillary fused to a laminate bract (as seen in *Rinistachya* and *Pseudobornia*), occasionally organised into fertile axes with determinate growth (strobili). This condition represents a plesiomorphic state, which either evolved toward complete fusion with the bract (as in Bowmanitaceae) or developed on fertile internodes instead of nodes, leading to the loss of the associated bract (as in Equisetales). Evolutionary convergences were also spotted between the *Peltastrobus-Lilpopia* clade and the equisetalean lineage, standing as the development of an equisetalean-like peltate shield per stalk (i.e. *Peltastrobus* and *Lilpopia*) and the loss fertile bracts (*Lilpopia*).

ACKNOWLEDGMENTS

Thanks are due to the following: Maurice Streel who helped in the redescription and identification of the spores of *Pseudobornia ursina;* Vivi Vajda and Stephen McLoughlin who provided a full access to the Nathorst, Antevs and Schweitzer collections. This study benefits from the support of the French Community of Belgium as part of the financing of a (FRS – FNRS) FRIA grant (No. FC63519).

REFERENCES

Antevs E, Nathorst AG. 1917: Kohlenfiihrende Kulm auf der Baren Insel. *Geologiska Foreningens i Stockholm Forhandlingar* 39, 649-663

Arnold CA. 1958. Petrified cones of the genus *Calamostachys* from the Carboniferous of Illinois. *Contributions from the Museum of Paleontology, University of Michigan* 14, 149–165.

Banks HP, Leclercq S, Hueber FM. 1975. Anatomyand morphology of *Psilophyton dawsonii*, sp. n. from the Late Lower Devonian of Quebec (Gaspé), and Ontario, Canada. *Palaeontographica Americana* 8, 77–125.

Bapst DW. 2012. paleotree: an R package for paleontological and phylogenetic analyses of evolution. *Methods in Ecology and Evolution* 3, 803–807.

Bateman R. 1991. Palaeobiological and phylogenetic implications of anatomically-preserved *Archaeocalamites* from the Dinantian of Oxroad Bay and Loch Humphrey Burn, southern Scotland. *Palaeontographica Abteilung B* 223, 1–59.

Baxter RW. 1972. A comparative study of nodal anatomy in *Peltastrobus reedae* and *Sphenophyllum plurifoliatum*. *Review of Palaeobotany and Palynology* 14, 41–47.

Bell MA, Lloyd GT. 2015. strap: an R package for plotting phylogenies against stratigraphy and assessing their stratigraphic congruence. *Palaeontology* 58, 379–389.

Berry CM, Edwards D. 1996b. *Anapaulia moodyi* gen. et sp. nov.: a probable iridopteridalean compression fossil from the Devonian of western Venezuela. *Review of Palaeobotany and Palynology* 93, 127 – 145.

Berry CM, Stein WE. 2000. A new iridopteridalean from the Devonian of Venezuela. *International Journal of Plant Sciences* 161, 807 – 827.

Berry CM, Stein WE, Cordi J. 2022. A New Reconstruction of the Iridopteridalean *Ibyka amphikoma* Skog et Banks from the Middle Devonian of Gilboa, New York State. *International Journal of Plant Sciences* 183, 450–464.

Boureau E. 1964. Traité de Paléobotanique. Tome II. Sphenophyta, Noeggerathiophyta. Masson et Cie, Paris, France.

Cariglino B. 2013. Fructification diversity from the La Golondrina Formation (Permian), Santa Cruz Province, Argentina. *Geobios* 46, 183–193.

Chu J, Durieux T, Tomescu AMF. 2024. An early cladoxylopsid with complex vascular architecture: *Paracladoxylon kespekianum* gen. et sp. nov. from the Lower Devonian (Emsian) of Quebec, Canada. *American Journal of Botany* 111, e16418.

Cúneo NR, Escapa I. 2006. The equisetalean genus *Cruciaetheca* nov. from the Lower Permian of Patagonia, Argentina. *International Journal of Plant Sciences* 167, 167–177.

Cutbill JL, Challinor A. 1965. Revision of the stratigraphical scheme for the Carboniferous and Permian rocks of Spitsbergen Bjørnøya. *Geological Magazine* 102, 418-439.

Dallmann WK, Gjelberg JG, Harland WB, Johannessen EP, Keilen HB, Lønøy A, Nilsson I, Worsley D. 1999. Lithostratigraphic lexicon of Svalbard. Review and recommendations

for nomenclature use. Upper Palaeozoic to Quaternary bedrock. *Norwegian Polar Institute Report* 318, 127–214.

D'Antonio MP, Hotton CL, Smith SY, Crane PR, Herrera F. 2024. Reconstruction of an enigmatic Pennsylvanian cone reveals a relationship to Sphenophyllales. *American Journal of Botany* 111, e16321.

Deng ZZ, Huang P, Liu L, Wang DM, Xue JZ. 2016. New observations of *Sphenophyllum pseudotenerrimum* Sze (Sphenopsida) from the Late Devonian of South China. *Acta Palaeontologica Sinica* 55 (1), 45– 55 (in Chinese, with English abstract)

Durieux T, Lopez MA, Bronson AW, Tomescu AMF. 2021. A new phylogeny of the cladoxylopsid plexus: contribution of an early cladoxylopsid from the Lower Devonian (Emsian) of Quebec. *American Journal of Botany* 108, 2066–2095.

Elgorriaga A, Escapa IH, Rothwell GW, Tomescu AMF, Rubén Cúneo N. 2018. Origin of *Equisetum*: Evolution of horsetails (Equisetales) within the major euphyllophyte clade Sphenopsida. *American Journal of Botany* 105, 1286–1303.

Galtier J, Daviero V. 1999. Structure and development of *Sphenophyllum oblongifolium* from the Upper Carboniferous of France. *International Journal of Plant Sciences* 160, 1021–1033.

Gelman A, Rubin DB. 1992. Inference from Iterative Simulation Using Multiple Sequences. *Statistical Science* 7, 457–472.

Goloboff PA, Catalano SA. 2016. TNT version 1.5, including a full implementation of phylogenetic morphometrics. *Cladistics* 32, 221–238.

Goloboff PA, Torres A, Arias JS. (2018). Weighted parsimony outperforms other methods of phylogenetic inference under models appropriate for morphology. *Cladistics* 34, 407–437.

Good CW. 1978. Taxonomic Characteristics of Sphenophyllalean Cones. *American Journal of*

Botany 65, 86–97.

Gothan W, Weyland H. 1973. *Lehrbuch der Paläobota*nik. 3rd edition. Berlin

Heer O. 1871. Die Mioziine Flora und Fatma Spitzbergens. *Kollgeliga Svenska Vetenskaps Akademiens Handlingar* 8. 7. Stockholm.

Hoffmeister WS, Staplin FL, Malloy RE. 1955. Mississippian plant spores from the Hardinsburg Formation of Illinois and Kentucky. *Journal of Paleontology*, 29, 372-399.

Holtedahl O. 1920. On the Palaeozoic Series of Bear Island, especially on the Heclahook system. *Norwegian Journal of Geology* 5, 121-148.

Huang P, Liu L, Deng Z, Basinger JF, Xue J. 2017a. *Xihuphyllum*, a novel sphenopsid plant with large laminate leaves from the upper Devonian of South China. *Palaeogeography, Palaeoclimatology, Palaeoecology* 466, 7–20.

Huang P, Liu Le, Liu Lu, Wang JS, Xue JZ. 2022. *Sphenophyllum* Brongniart (Spheno- psida) from the Upper Devonian of South China. *Palaeoworld* 31, 402–418.

Huelsenbeck JP, Ronquist F. 2001. MRBAYES: Bayesian inference of phylogenetic trees. *Bioinformatics* 17, 754–755.

Janocha J, Wesenlund F, Thießen O, Grundvåg SA, Koehl JB, Johannessen EP. 2024. Depositional environments and source rock potential of some Upper Palaeozoic (Devonian) coals on Bjørnøya, Western Barents shelf. *Marine and Petroleum Geology* 163, 106768.

Kassambara A. 2017. *Practical Guide To Principal Component Methods in R: PCA, M(CA), FAMD, MFA, HCPC, factoextra*. STHDA.

Kenrick P, Crane PR. 1997. *The origin and early diversification of land plants*. Washington: Smithsonian Institution Press.

Kerp H. 1984. Aspects of Permian palaeobotany and palynology. III. A new reconstruction of *Lilpopia raciborskii* (Lilpop) Conert et Schaarschmidt (Sphenopsida). *Review of*

Palaeobotany and Palynology 40, 237–261.

King B. 2021. Bayesian Tip-Dated Phylogenetics in Paleontology: Topological Effects and Stratigraphic Fit. *Systematic Biology* 70(2): 283–294.

Leclercq S. 1957. *Etude d'une fructification de Sphenopsida à structure conservée du Devonian supérieur.* Mémoires, L'Académie Royal de Belgique, Classe des Sciences, Collection 14, 1- 39.

Leclercq S, Banks HP. 1962. *Pseudosporochnus nodosus* sp. nov., a Middle Devonian plant with cladoxylalean affinities. *Palaeontographica Abteilung B* 110, 1–34.

Leclercq S. 1969. *Calamophyton primaevum*: The Complex Morphology of Its Fertile Appendage. *American Journal of Botany* 56, 773–781.

Leisman GA, Graves C. 1964. The Structure of the Fossil Sphenopsid Cone, *Peltastrobus reedae*. *American Midland Naturalist* 72, 426–437.

Levittan ED, Barghoorn ES. 1948. *Sphenostrobus thompsonii*: A New Genus of the Spenophyllales? *American Journal of Botany* 35, 350–358.

Lewis PO. 2001. A Likelihood Approach to Estimating Phylogeny from Discrete Morphological Character Data. *Systematic Biology* 50, 913–925.

Li X, Cai C, Wang Y. 1995. *Hamatophyton verticillatum* (Gu and Zhi) emend. A primitive plant of sphenopsida from the upper Devonian- lower carboniferous in China. *Palaeonto-graphica Abteilung B: Palaeophytologie* 235, 1–22.

Libertín M, Bek J, Drábková J. 2014. New sphenophyllaleans from the Pennsylvanian of the Czech Republic. *Review of Palaeobotany and Palynology* 200, 196–210.

Libertín M, Bek J, Wang J, Opluštil S, Pšenička J, Frojdová, JV. 2021. New data about three sphenophylls and their spores from the volcanic tuff of Wuda, Taiyuan Formation, earliest Permian, China. *Review of Palaeobotany and Palynology* 294, 104484.

Lilpop J. 1937. New plants from the Permo-carboniferous rocks in Poland. *International*

Bulletin of the Polish Academy of Sciences and Letters: Mathematical and Natural Sciences Class: Series B: Natural Sciences 1, 1– 10

Lipiarski I. 1971. La flore du Permien inférieur apparaissant dans le travertin de Karniowice aux environs de Cracovie. *Prace - Panstwowego Instytutu Geologicznego* 58, 5–112.

Lipiarski I. 1972a. New data concerning the morphology of the fossil genus *Lilpopia* Conert et Schaarschmidt 1970 (= *Tristachya* Lilpop 1937). *Acta Palaeobotanica* 13(2), 101–109.

Liu L, Pšenička J, Bek J, Wan M, Pfefferkorn HW, Wang J. 2021. A whole calamitacean plant *Palaeostachya guanglongii* from the Asselian (Permian) Taiyuan Formation in the Wuda Coalfield, Inner Mongolia, China. *Review of Palaeobotany and Palynology* 294, 104245.

Luo A, Duchêne DA, Zhang C, Zhu C, Ho SYW. 2020. A Simulation-Based Evaluation of Tip-Dating Under the Fossilized Birth–Death Process. *Systematic Biology* 69 (2), 325-344.

Mosbrugger V. 1990. The Tree Habit in Land Plants: a Functional Comparison of Trunk Constructions with a Brief Introduction into the Biomechanics of Trees. *Journal of Evolutionary Biology* 4, 516-517.

Nathorst AG. 1894. Zur paläozoischen Flora der arktischen Zone der Bäreninsel. *Svenska Veten· skaps Akademiens Handlingar* 26(4), 1–80.

Nathorst AG. 1902. Zur oberdevonischen Flora der Bäreninsel. *Svenska Veten· skaps Akademiens Handlingar* 36(3), 1–60.

Neuberg MF. 1964. Permian flora of the Petchora Basin, part II. Sphenopsida [in Russian]. *Trudy Geologicheskogo Instituta Akademii Nauk SSSR* 30, 1–90.

Orlova OA, Jurina AL. 2014. A new articulate species, *Pseudobornia schweitzeri* Jurina et O. Orlova, sp. nov., from the Upper Devonian of Northern Timan, Russia. *Paleontological Journal* 48, 90–100.

Prestianni C, Gess RW. 2019. *Rinistachya hilleri* gen. et sp. nov. (Sphenophyllales), from the

upper Devonian of South Africa. *Organisms Diversity & Evolution* 19(1), 1–11.

R Core Team. 2022. R: A language and environment for statistical computing. v. 4.2.1. R Foundation for Statistical Computing, Vienna, Austria. Website https://www.R-project.org/.

Rothwell GW. 1999. Fossils and ferns in the resolution of land plant phylogeny. *Botanical Review* 65, 188–218.

Rothwell GW, Taylor TN. 1971a. Studies of Paleozoic calamitean cones: *Weissia kentuckiense* gen. et sp. nov. *Botanical Gazette* 132, 215–224.

Rothwell GW, Taylor TN. 1971b. *Weissistachys kentuckiensis*: a new name for *Weissia kentuckiense* Rothwell and Taylor. *Botanical Gazette* 132, 371–372.

Schweitzer HJ. 1967. Die Oberdevon Flora der Bäreninsel: 1. *Pseudobornia ursina* Nathorst, *Palaeontographica Abteilung B: Palaeophytologie* 120, 116–137.

Schweitzer HJ. 1990. Pflanzen erobern das Land. *Kleine Senckenberg-Reihe Frankfurt am Maine* 18, 1–75.

Schweitzer HJ. 2003. Die Landnahme der Pflanzen, *Decheniana (Bonn)* 156, 177–215.

Schweitzer HJ. 2006. Die Oberdevon-Flora der Bäreninsel - 5. Gesamtübersicht. *Palaeontographica Abteilung B: Palaeophytologie* 274, 1–191.

Simões T, Greifer N, Barido-Sottani J, Pierce S. 2023. EvoPhylo: An r package for pre- and postprocessing of morphological data from relaxed clock Bayesian phylogenetics. *Methods in Ecology and Evolution*.

Skog J, Banks HP. 1973. *Ibyka amphikoma*, gen. Et sp. nov., a new protoarticulate precursor from the late middle Devonian of New York state. *American Journal of Botany* 60, 366–380.

Stein WE, Wight DC, Beck CB. 1984. Possible Alternatives for the Origin of Sphenopsida. *Systematic Botany* 9, 102–118.

Stewart WN, Rothwell GW. 1993. Paleobotany and the evolution of plants. *Cambridge University Press*, Cambridge, UK.

Streel M. 2009. Upper Devonian miospore and conodont zone correlation in western Europe. *Geological Society Special Publication* 314, 163–176.

Stur D. 1875. Die Culm-Flora des Mährisch-Schlesischen Dachschiefers. *Abhandlungen der kaiserlich-königlichen geologischen Reichsanstalt* 8, 1–106.

Stur D. 1877. Die Culm-Flora der Ostrauer und Waldenburger Schichten. *Abhandlungen der kaiserlich-königlichen geologischen Reichsanstalt* 8, 1–366.

Taylor TN. 1970. The Morphology of *Bowmanites dawsoni* Spores. *Micropaleontology* 16, 243–248.

Taylor TN, Taylor EL, Krings M. 2009. *Paleobotany. The biology and evolution of fossil plants*, 2nd ed. Academic Press, Amsterdam, Netherlands.

Tomescu AMF, Escapa IH, Rothwell GW, Elgorriaga A, Cúneo NR. 2017. Developmental programmes in the evolution of *Equisetum* reproductive morphology: a hierarchical modularity hypothesis. *Annals of Botany* 119, 489–505.

Tomescu AMF, Whitewoods C. 2024. Development on the rocks: Integrating molecular biology and the fossil record to reconstruct the evolution of leaf development. *Perspectives in Plant Ecology, Evolution and Systematics* 64, 125797.

Wang Z, Geng B. 1997. A new Middle Devonian plant: *Metacladophyton tetraxylum* gen. et sp. nov. *Palaeontographica Abteilung B: Palaeophytologie* 243, 85-102.

Wang DM. 2008. A new iridopteridalean plant from the middle Devonian of Northwest China. *International Journal of Plant Sciences* 169, 1100–1115.

Wang D, Guo Y. 2009. *Hamatophyton* from the Late Devonian of Anhui Province, South China and Evolution of Sphenophyllales. *Acta Geologica Sinica* 83, 492–503.

Wang DM, Hao SG, Wang Q. 2005. *Rotafolia songziensis* gen. et comb. nov., a sphenopsid

from the Late Devonian of Hubei, China. *Botanical Journal of Linnean Society* 148, 21–37.

Wang D, Hao S, Tian L, Xue J. 2006. Further Study of the Late Devonian Sphenopsid *Hamatophyton verticillatum* from China. *International Journal of Plant Sciences* 167, 885–896.

Worsley D, Edwards MB. 1976. The Upper Palaeozoic succession of Bjørnøya, *Norsk Polarinst. Arbok* 314, 163-176.

Worsley D, Agdestein T, Gjelberg JG, Kirkemo K, Mørk A, Nilsson I, Olaussen S, Steel RJ, Stemmerik L. 2001. The geological evolution of Biørnøya, Arctic Norway: implications for the Barents Shelf. *Norwegian Journal of Geology* 81, 195–234.

Ziegler PA. 2012. *Evolution of Laurussia: A Study in Late Palaeozoic Plate Tectonics.* Springer Science & Business Media.

Figure captions

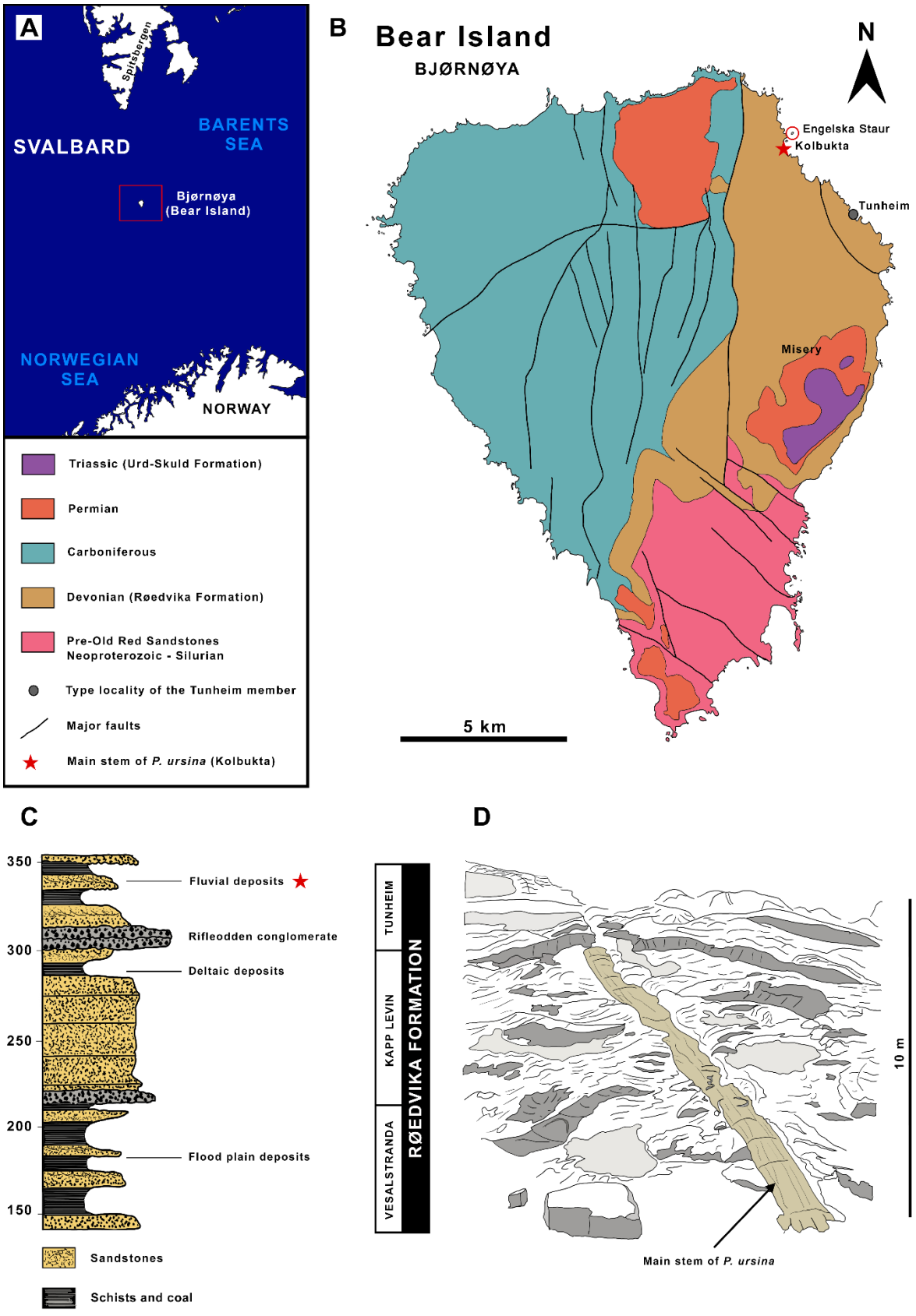

Figure 1: Geological context of the studied locality at Bear Island (Bjørnøya). A, Geographic position of Bear Island (Norway) within the Barents Sea. B, Simplified geological map of Bear Island adapted from Dallmann (1999). C, Simplified lithostratigraphic column of the Røedvika Formation based on Worsley *et al*. (2001). D, Sketch of the inner-cast of the trunk-like stem of *Pseudobornia ursina* outcropping in the sandstones of the Kolbukta (Tunheim member) based on the field photography from Schweitzer (2006): page 79, fig. 36.

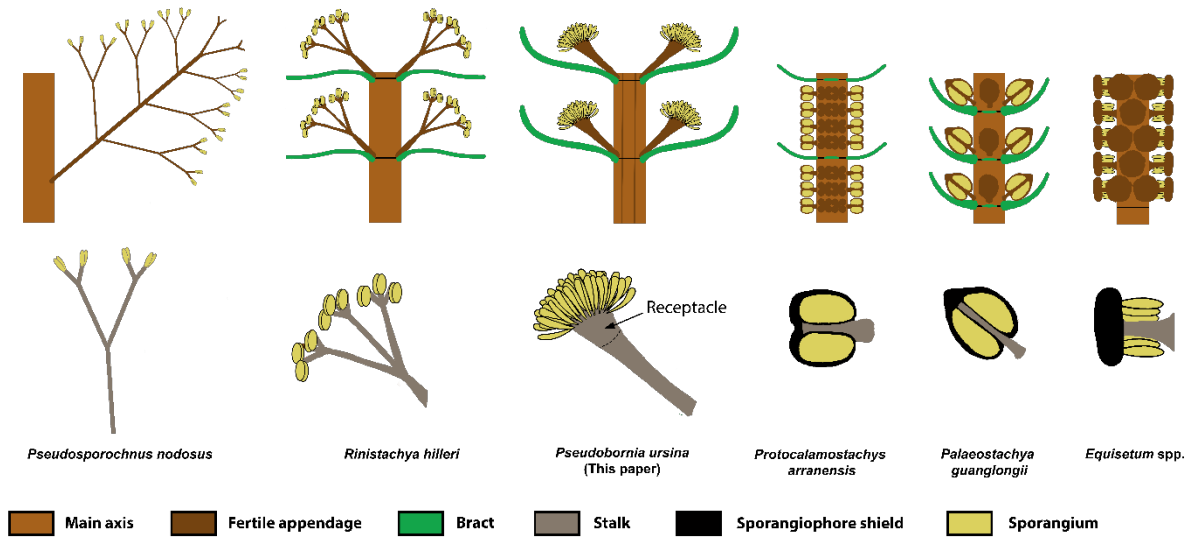

Figure 2: Schematic architectural models showing differences in fertile units (top) and appendages (bottom) of selected sphenopsids and cladoxylopsids, illustrating the terminology used in this study. *Pseudosporochnus nodosus* after Leclercq and Banks (1962); *Rinistachya hilleri* after Prestianni & Gess (2019); *Pseudobornia ursina* (this work); *Protocalamostachys arranensis* after Bateman (1991); *Palaeostachya guanglongii* after Liu *et al.* (2017).

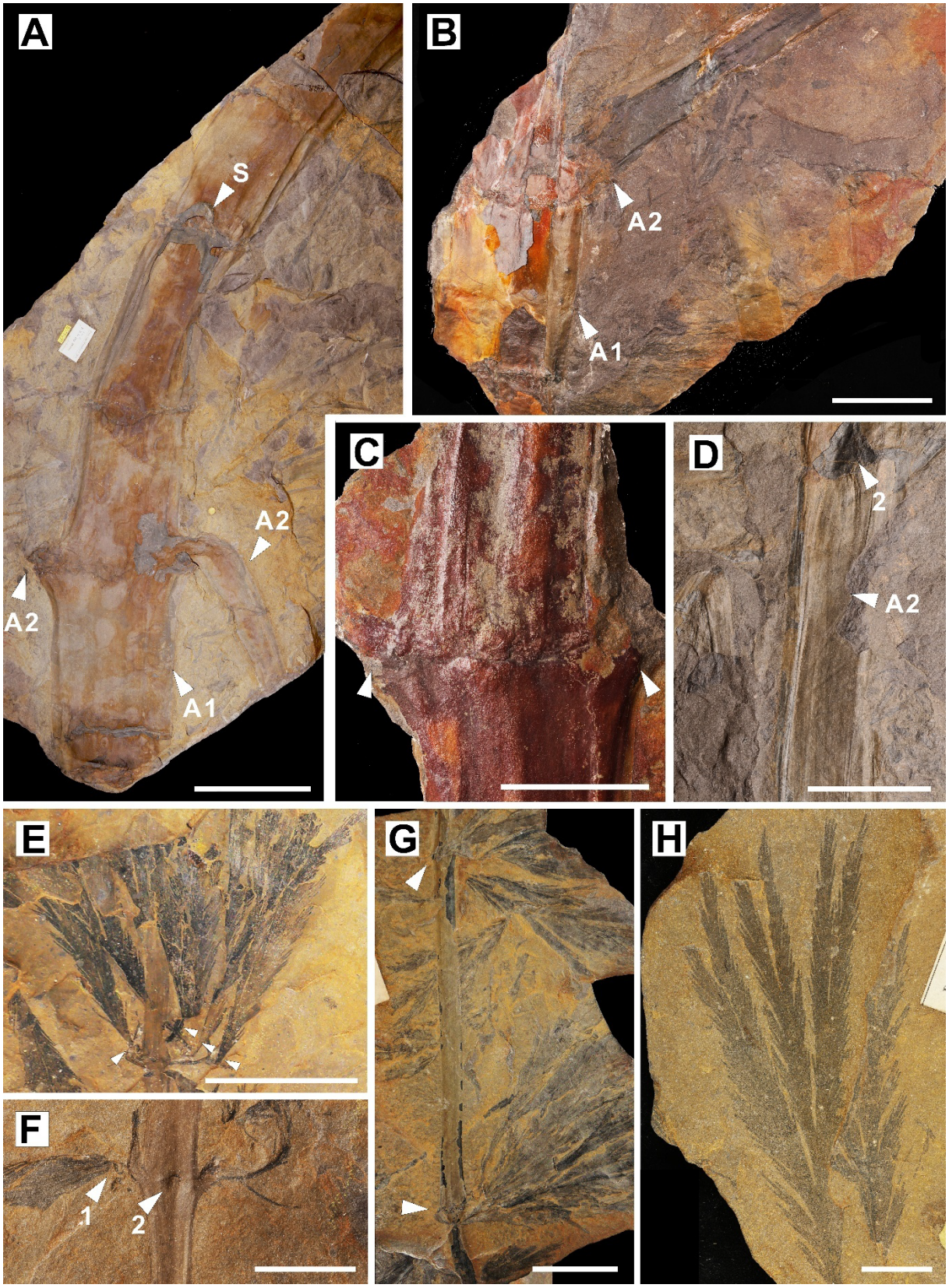

Figure 3: Vegetative parts of *Pseudobornia ursina* sampled on Bjørnøya (Norway), belonging to the Schweitzer and Nathorst collections (Naturhistoriska riksmuseet). A, Trunk-like stem of *P.*

ursina (A1) displaying five curved nodal lines. At the second node, two second-order axes are inserted (A2), while the fourth node bears an oval-shaped branch scar; S038058. Scale bar = 10 cm. B, Trunk-like stem of *P. ursina* (A1) on which is inserted a second order axis (A2); JE-Sch0181. C, Trunk-like stem of *P. ursina* (A1) with a curved nodal line on which is inserted two second order axes (at arrows); JE-Sch0071. D, Second order axis that displays longitudinal and continuous ribs (arrow 1) and a 3rd order branch scar (arrow 2); JE- Sch0077. Scale bars = 5 cm. E, Last order axis bearing whorls of four fimbriate leaves; S021000. Scale bar = 5 cm. F, Last order axis bearing nodal whorl of fimbriate leaves (1) and a leaf scar (2); S038054. Scale bar = 1 cm. G, Last order axis bearing whorls of four fimbriate leaves (arrows); S038068. Scale bar = 2 cm. H, Detached fimbriate leaves of *Pseudobornia*; S038050. Scale bar = 1 cm.

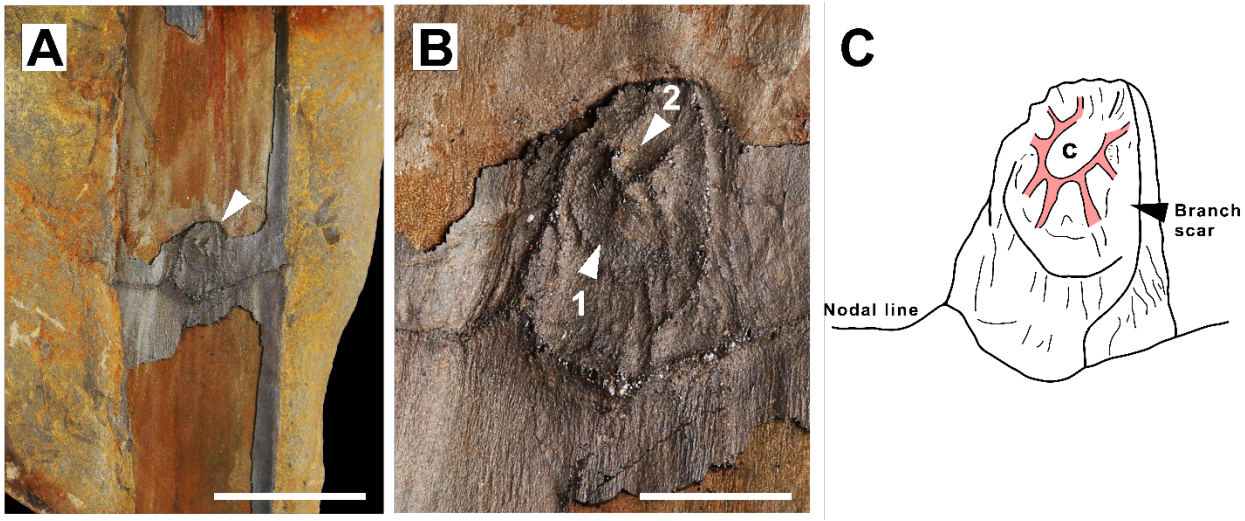

Figure 4: Vegetative second order axis of *Pseudobornia ursina* that displays a third order branch scar, sampled on Bjørnøya (Norway), belonging to the Schweitzer collections (Naturhistoriska riksmuseet). A, Second order axis (A2) that displays a 3rd order branch scar (arrow); JE-Sch0067-01. Scale bar = 2 cm. B, Detailed view of the branch scar exhibiting radially arranged ridges (1) surrounding the medullary canal (2); JE-Sch0067-01. Scale bar = 0.5 cm. C. Line drawing of the branch scar with radially arranged ridges interpreted as vascular bundles(highlighted in red), surrounding the medullary cavity (c).

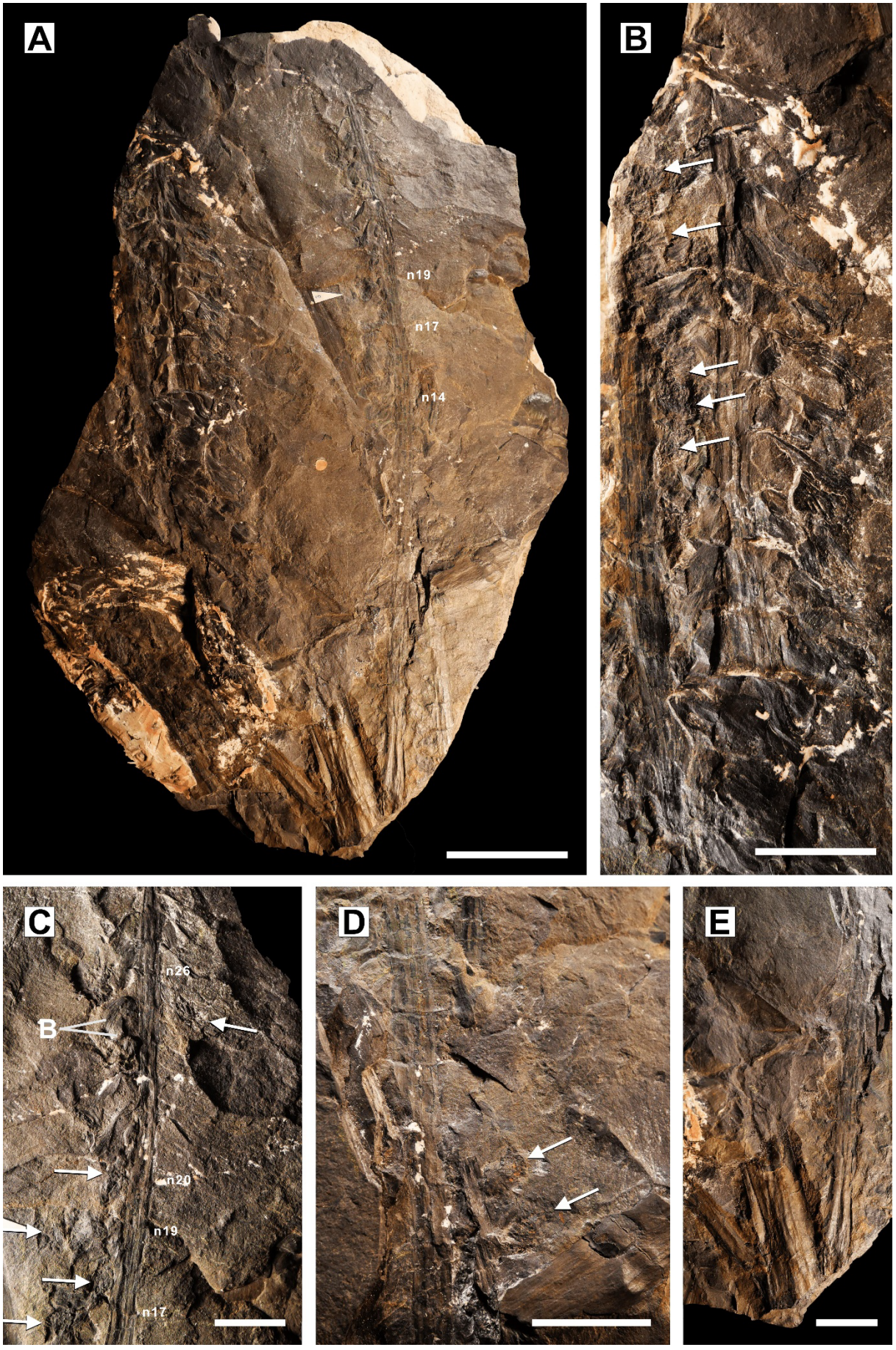

1

Figure 5: Photographs of the fertile specimen of *Pseudobornia ursina* (S038066) found at Kolbukta by Nathorst (1902), displaying seven different fertile axes or strobili. A, General view of the fertile specimen. Scale bar = 5 cm. B, Fertile axes #1 and #2, arrows indicate the fertile appendage. Scale bar = 2 cm. C, Fertile axis #4, arrows indicate the fertile appendages. Scale bar = 2 cm. D, Fertile axes #4 and #5, arrows indicate the fertile appendages. Scale bar = 2 cm. E, Nodal insertion of the 4^{th} axis; sp. a. Scale bar = 2 cm. B = bisected bract.

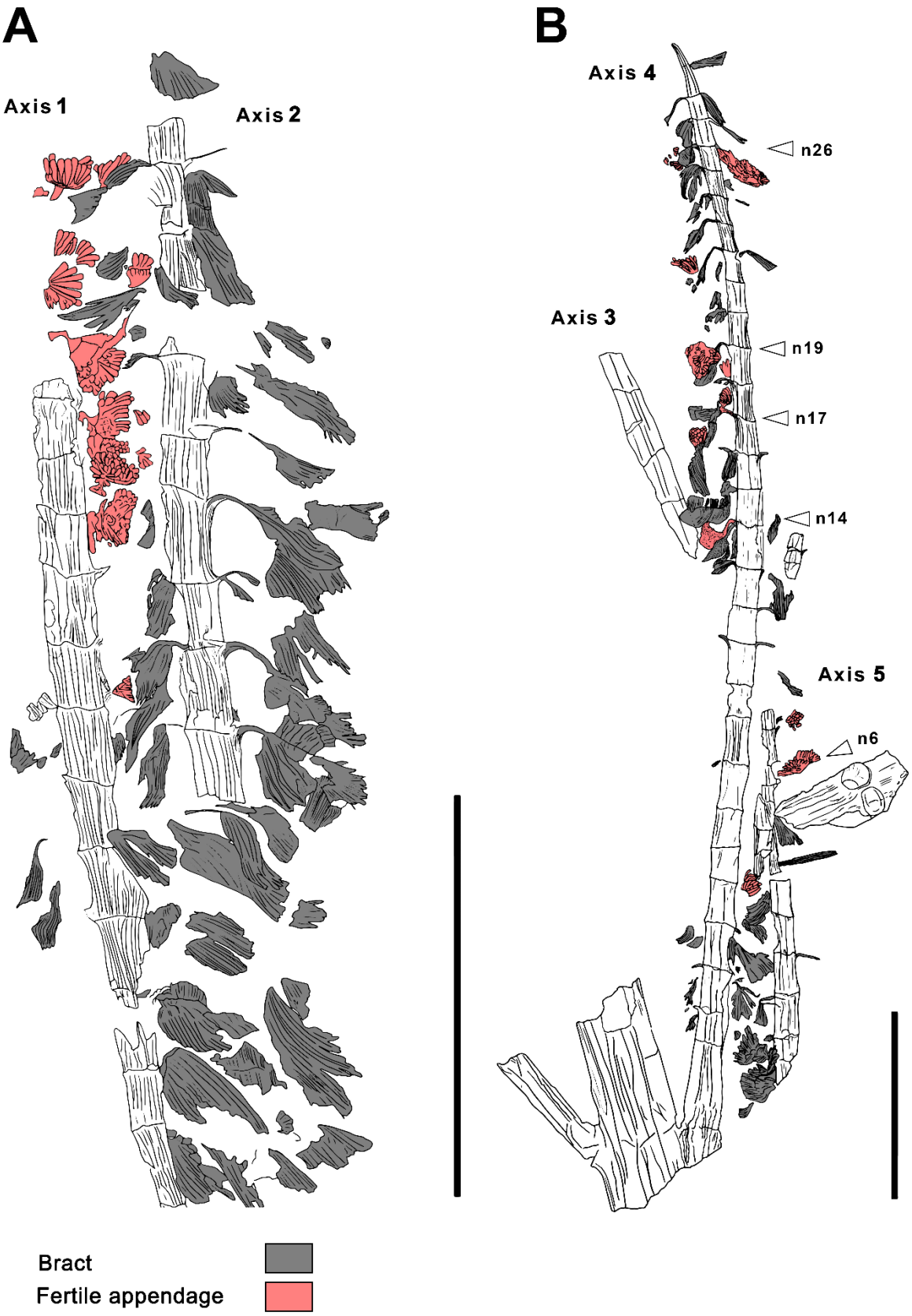

Figure 6: Line drawing of the fertile axes #1 to #5 with their associated fertile appendages and bracts; sp. a. A, Sketch of the paired axes #1 and #2. B, Sketch of the 3rd, 4th, and 5th axes. Scale

bars = 5 cm.

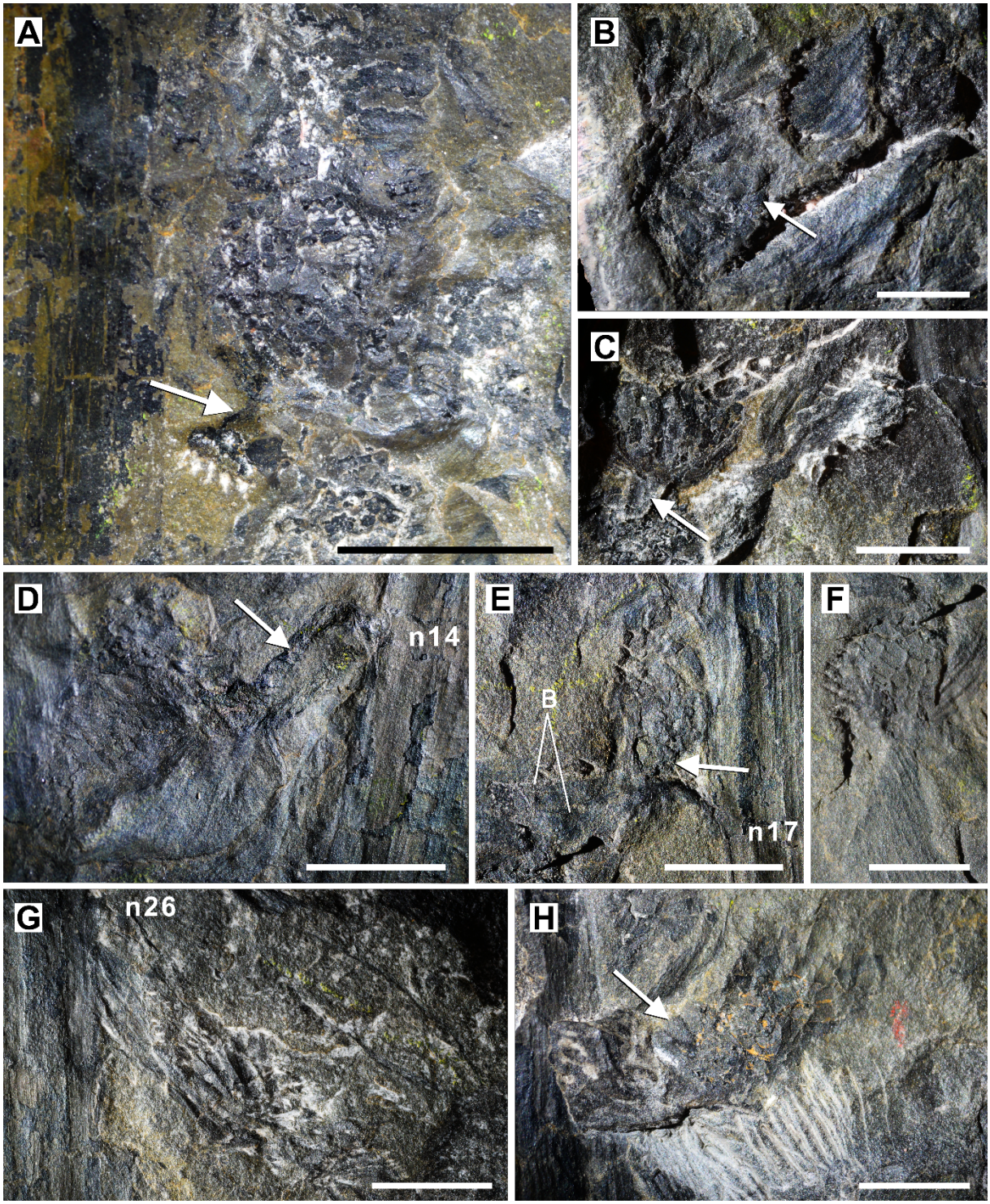

Figure 7: Detailed view of the fertile units of *Pseudobornia ursina*; sp. a. A, Detached fertile appendages alongside the third axis with its stalk (arrow). B, Detached fertile part (above the axis #1) showing elongated and radially inserted sporangia (arrow). C, Detached fertile part

(above the axis #1) showing the upper part of its stalk (arrow) as well as radially inserted sporangia. D, Nearly intact bract inserted on the 14th node (axis #4) that subtends a massive fertile appendage inserted through its long stalk (arrow) to the leaf axil. E, Damaged bract inserted on the 17th node (axis #4) that subtends a compact fertile appendage showing a partly hidden stalk (arrow). F, Damaged bract and the associated fertile part, which is compressed from the top (axis #4). G, Fertile appendage and its stalk inserted on the 26th node of the sixth axis. H, Laterally compressed fertile appendage alongside the seventh axis, the arrow indicates a sporangium. Scale bars = 5 mm. B = bifurcated bract.

	Axis 1	**Axis 2**	**Axis 3**	**Axis 4**	**Axis 5**	**Axis 6**
Total length on average (cm)	11,0	8,5	6,3	32,0	10,1	7,8
Length of internode on average (cm)	1,1	1,1	/	0,93	0,9	0,88
Apex preserved	absent	absent	absent	present	absent	absent
Attachment to the main stem	absent	absent	absent	present	absent	absent
Num. of bracts	~30		/	~30	5	~10
Num. of attached bracts	0	8	/	15	1	4
Bracts with entire margins	absent	absent	absent	present	absent	present
Nodes of interest (n)	/	/	/	14, 17, 19	/	4, 5, 7, 8
Evidence of bisected bracts	absent	present	Absent	present	absent	absent
Nodes of interest (n)	/	3	/	17, 25	/	/
Num. of fertile appendages (F.a)	8		0	7	3	3
Num. of F.a with stalk	4 (partially preserved)		/	2	/	2 to 3
Nodes of interest (n)	along axis 1 and 2		/	14, 26	/	4, 5, 7?
Num. of still attached F.a	/		/	3 to 4	/	2
Elongated sporangia preserved	present		absent	absent	present	absent

Table 1: Summary and comparison of morphological features observed in each individual strobilus. See Fig. 6 for axis localization, illustrations, and detailed features of bracts and fertile appendages.

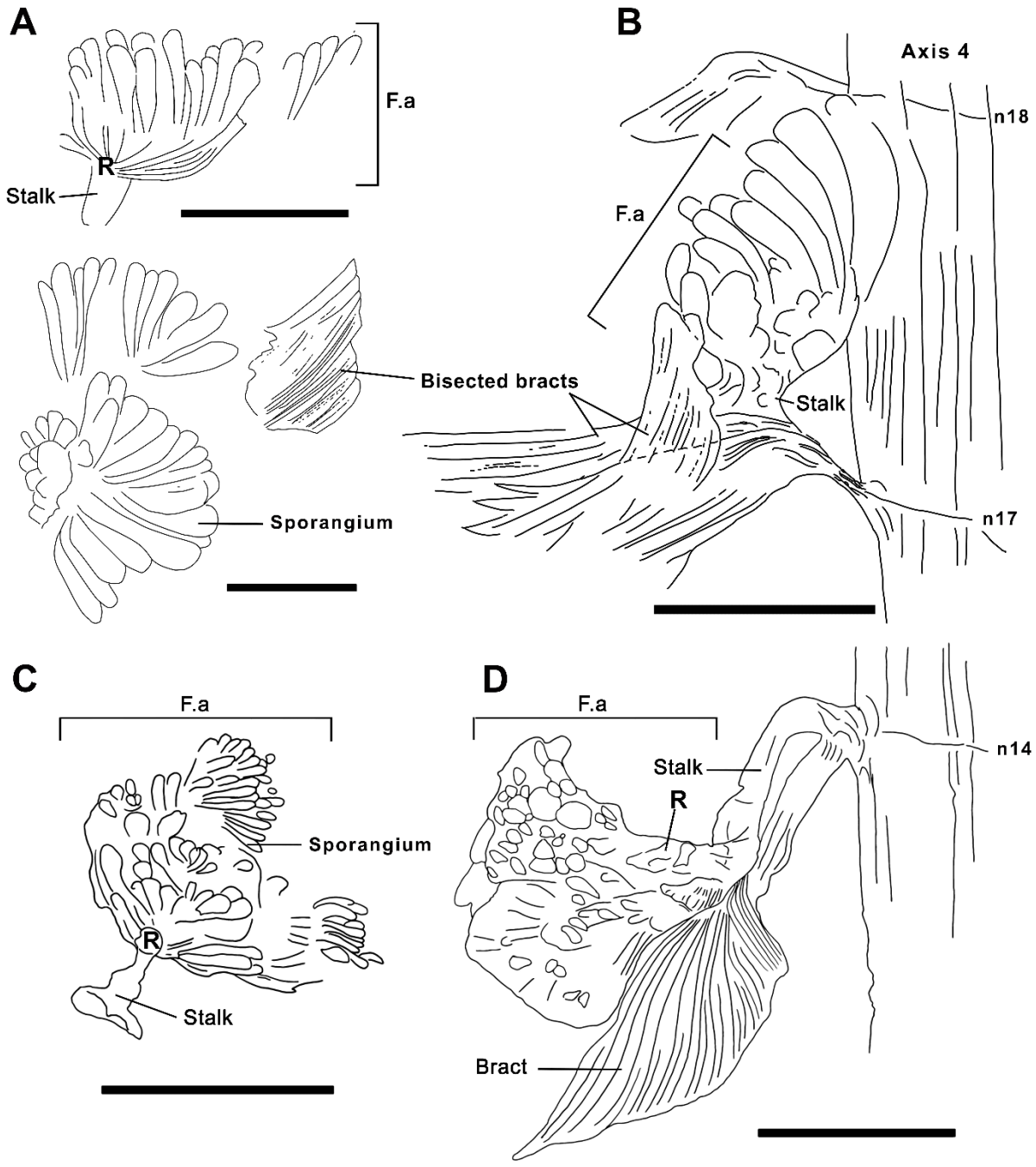

Figure 8: Line drawings of selected fertile appendages, sporangia and bracts along the first and fourth axis. A, Detached fertile appendages showing elongated and radially inserted sporangia (above the axis #1). B, Damaged bract inserted on the 17th node that subtends a compact fertile appendage showing a partly hidden stalk (axis #4). C, Detached fertile appendages alongside the first axis, displaying its broken stalk. D, Nearly intact bract inserted on the 14th node that subtends a massive fertile appendage inserted through its long stalk to the leaf axil (axis #4).

Scale bars = 5 mm. F.a = Fertile appendages; R = Receptacle.

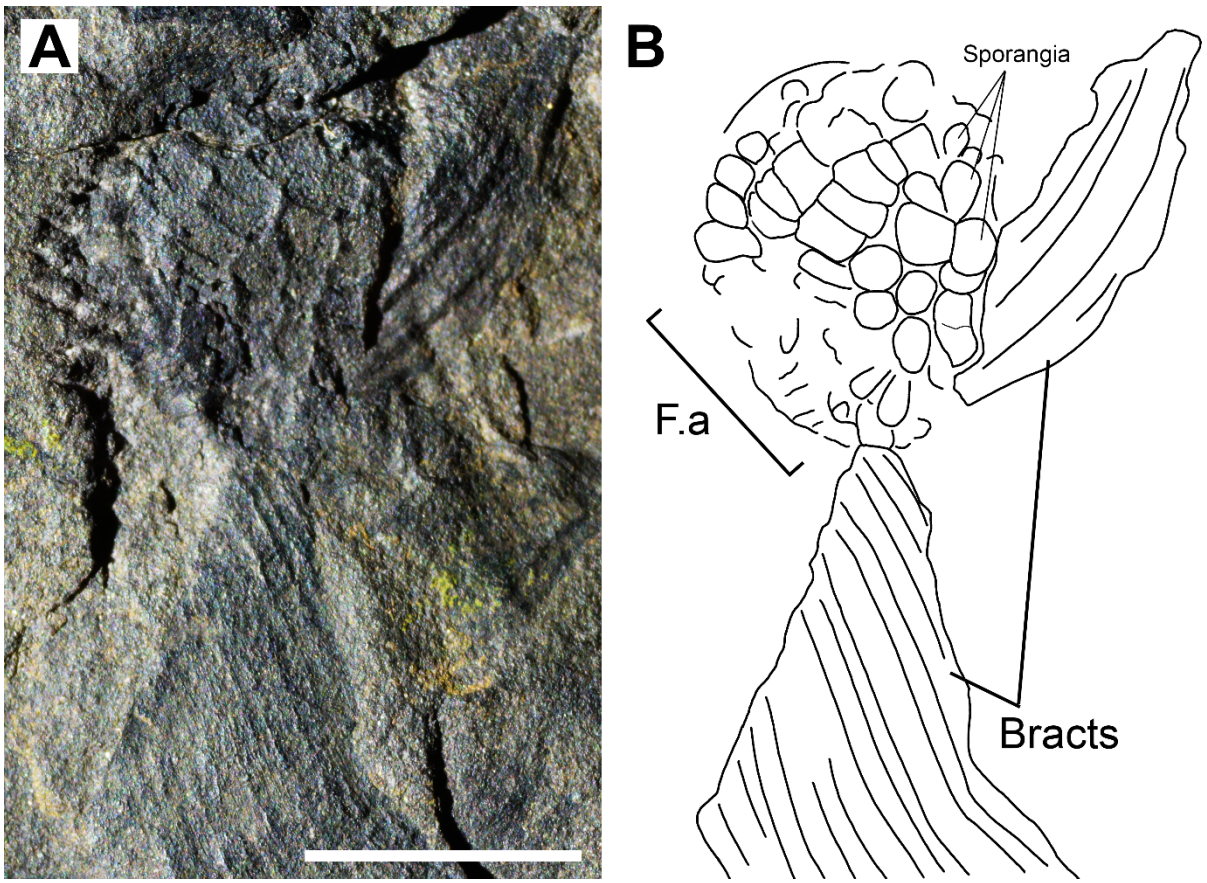

Figure 9: Fertile appendage and associated line drawing showing the organisation of sporangia inserted on the receptacle, found along the axis #4, at node 16. A, Fertile appendage exhibiting circles of compressed sporangia. B, Line drawing of the compressed fertile appendage + associated damaged bracts. Scale bar = 5 mm. F.a = Fertile appendage.

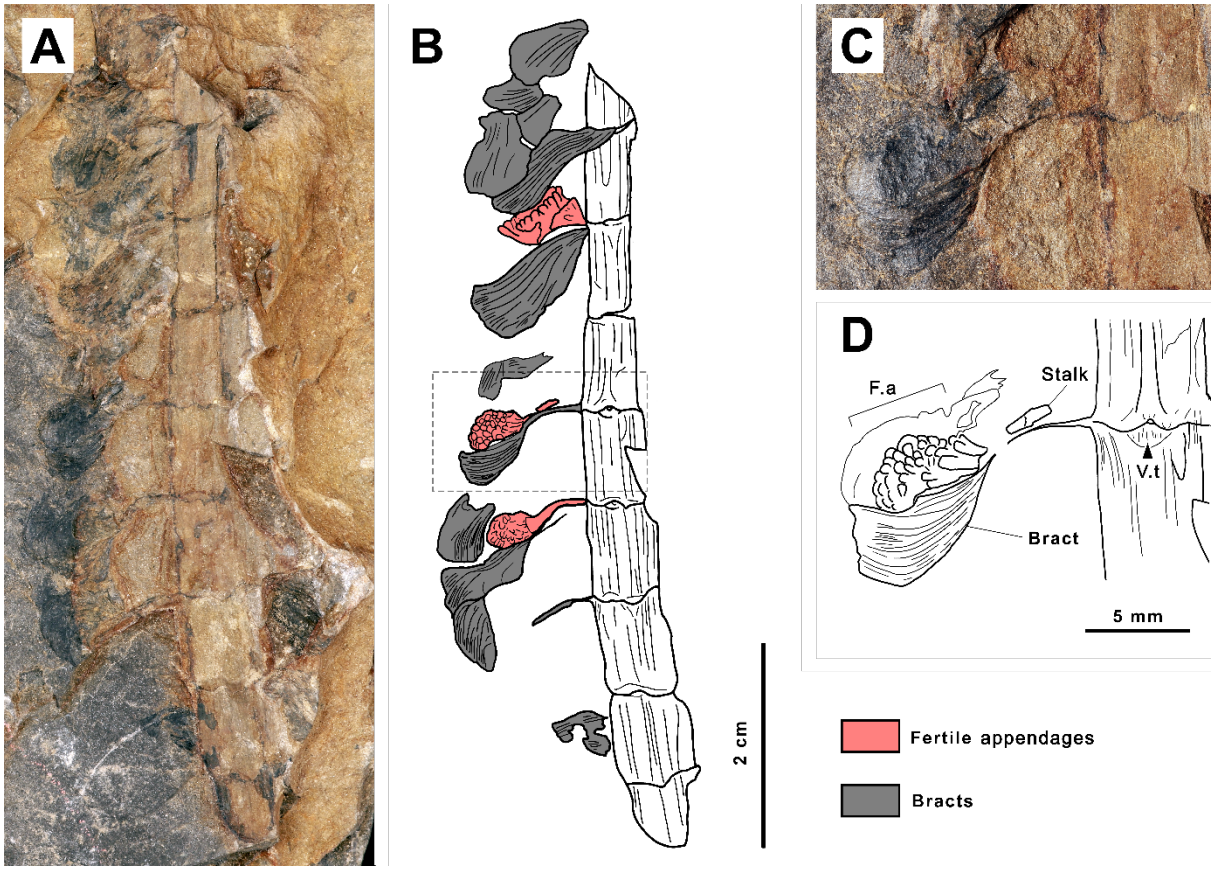

Figure 10: The second, newly identified, fertile specimen of *Pseudobornia ursina* (S038344) found in Engelska Staur by Antevs (1916) displaying one incomplete fertile axis. A, General view of the fertile axis; S038344. B, Line drawing of the fertile axis #6 with their associated fertile appendages and bracts. C, 4th fertile node displaying a compact fertile appendage subtended by its bract and a frontal vascular trace (fertile appendage + bract scar). D, Line drawing of the 4th fertile node. V.t = Vascular trace; F.a = Fertile appendages.

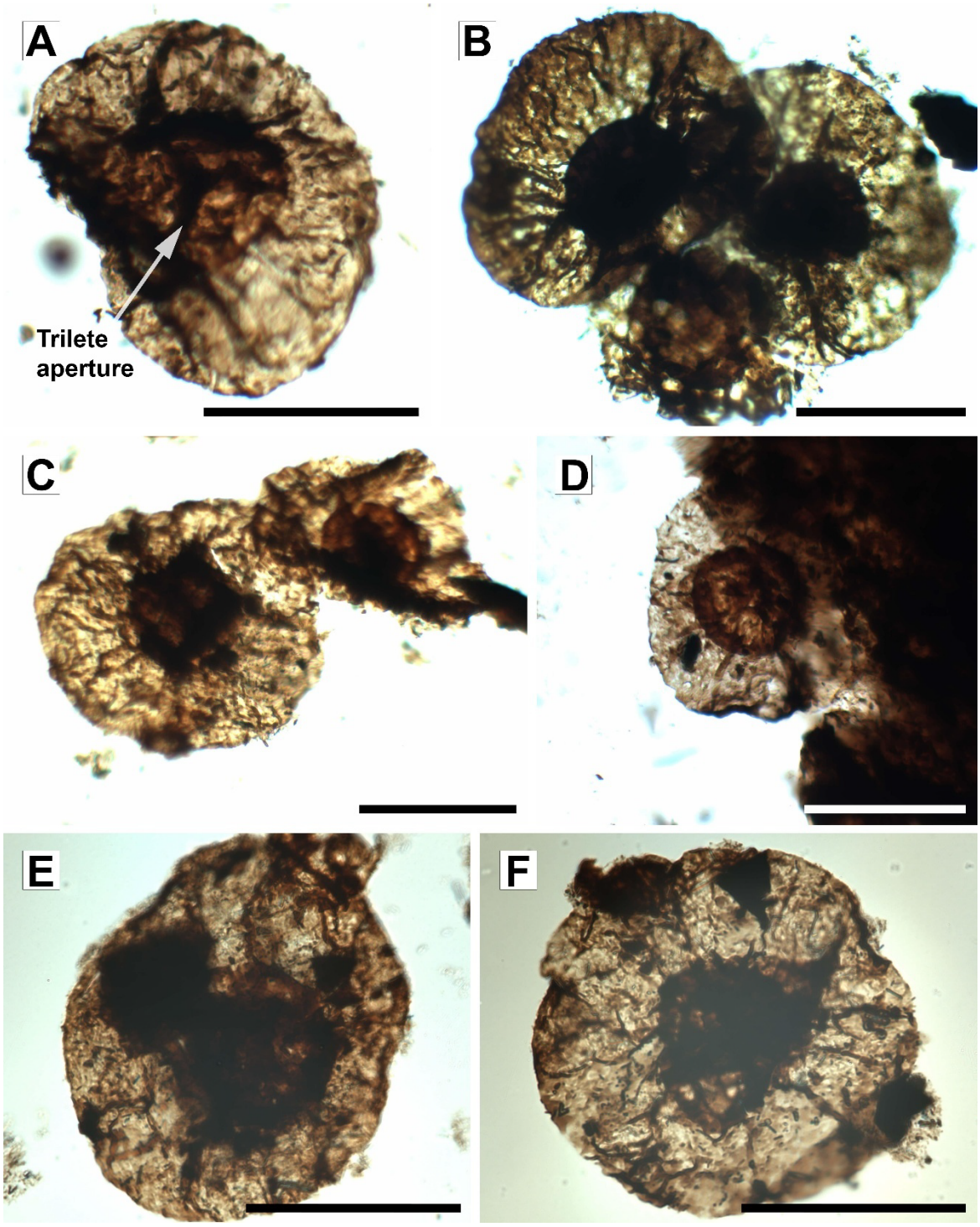

Figure 11: Selected *in-situ* spores of *Pseudobornia ursina* in polar view sampled in the specimen S038066. A, Spore with a visible trilete scar. B, Damaged circular spores within a cluster. C, Damaged circular spores within a cluster, showing a slightly visible trilete scar. D, Subcircular spore with its trilete scar confined to the intexine. E, Spore with a circular amb and a triangular core. F, Spore with a circular amb and a triangular core. Scale bars = 100 µm.

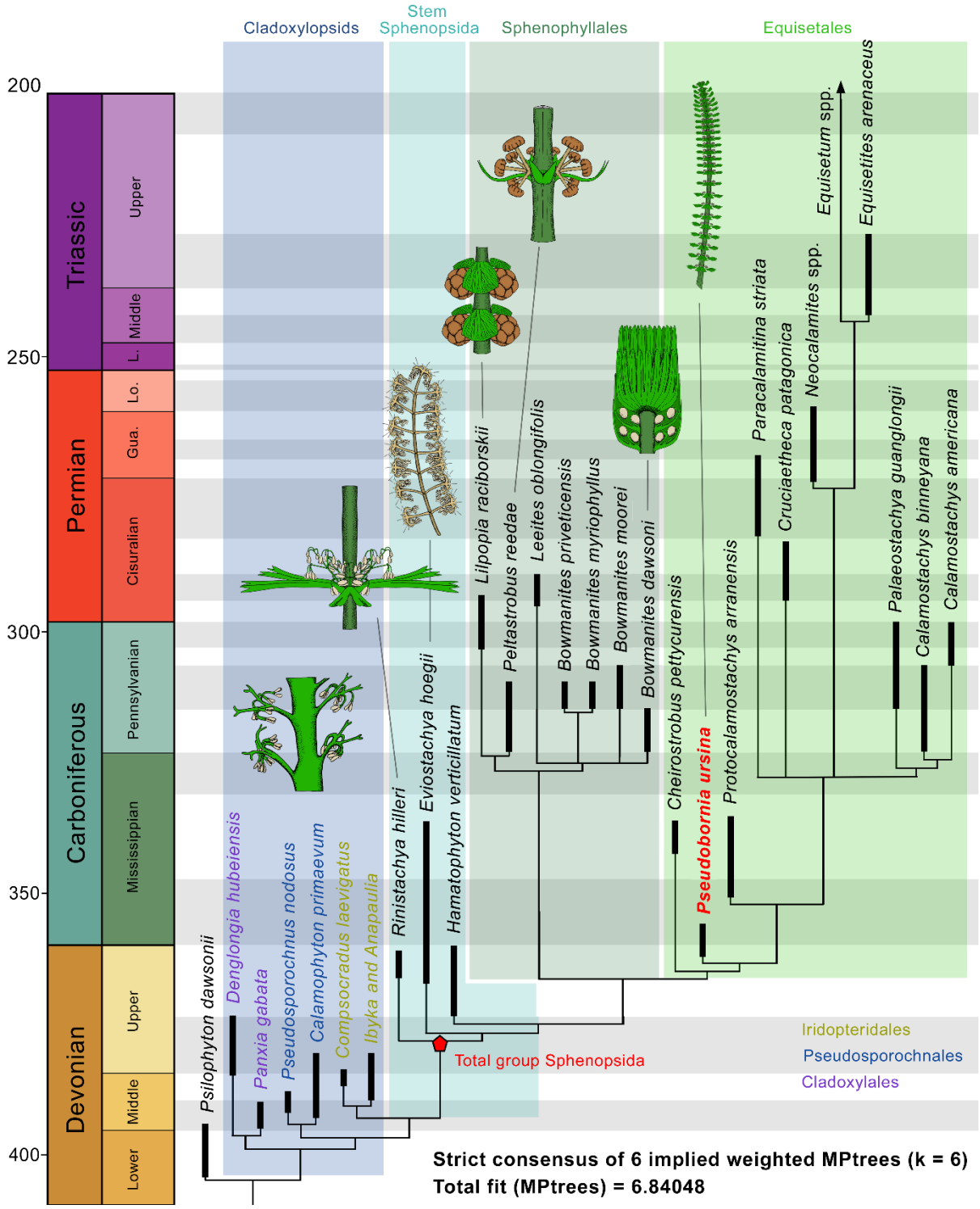

Figure 12: Relationships among sphenophytes and cladoxylopsids based on morphological evidence. The topology shown corresponds to the strict consensus tree based on 6 most parsimonious trees obtained from an implied weighted maximum parsimony analysis with a concavity value of 6. Total fit of MPtrees = 6.84048.

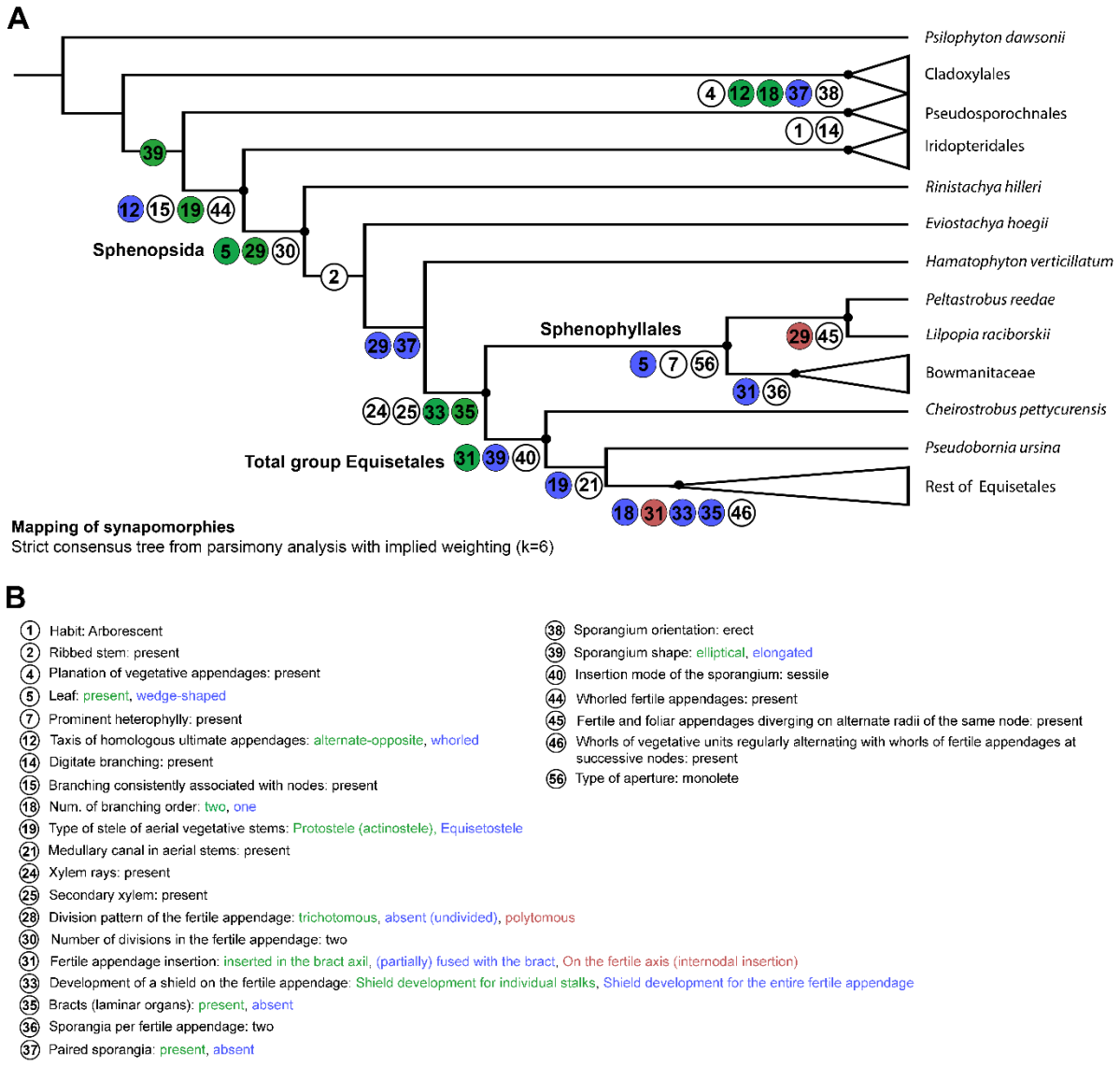

Figure 13: Synapomorphies mapped on the abridged strict consensus tree resulting from parsimony-based analyses with implied weights (k = 6, 9 and 12). (A) Tree depicting overall relationships obtained from our matrix of characters. (B) Characters and states.

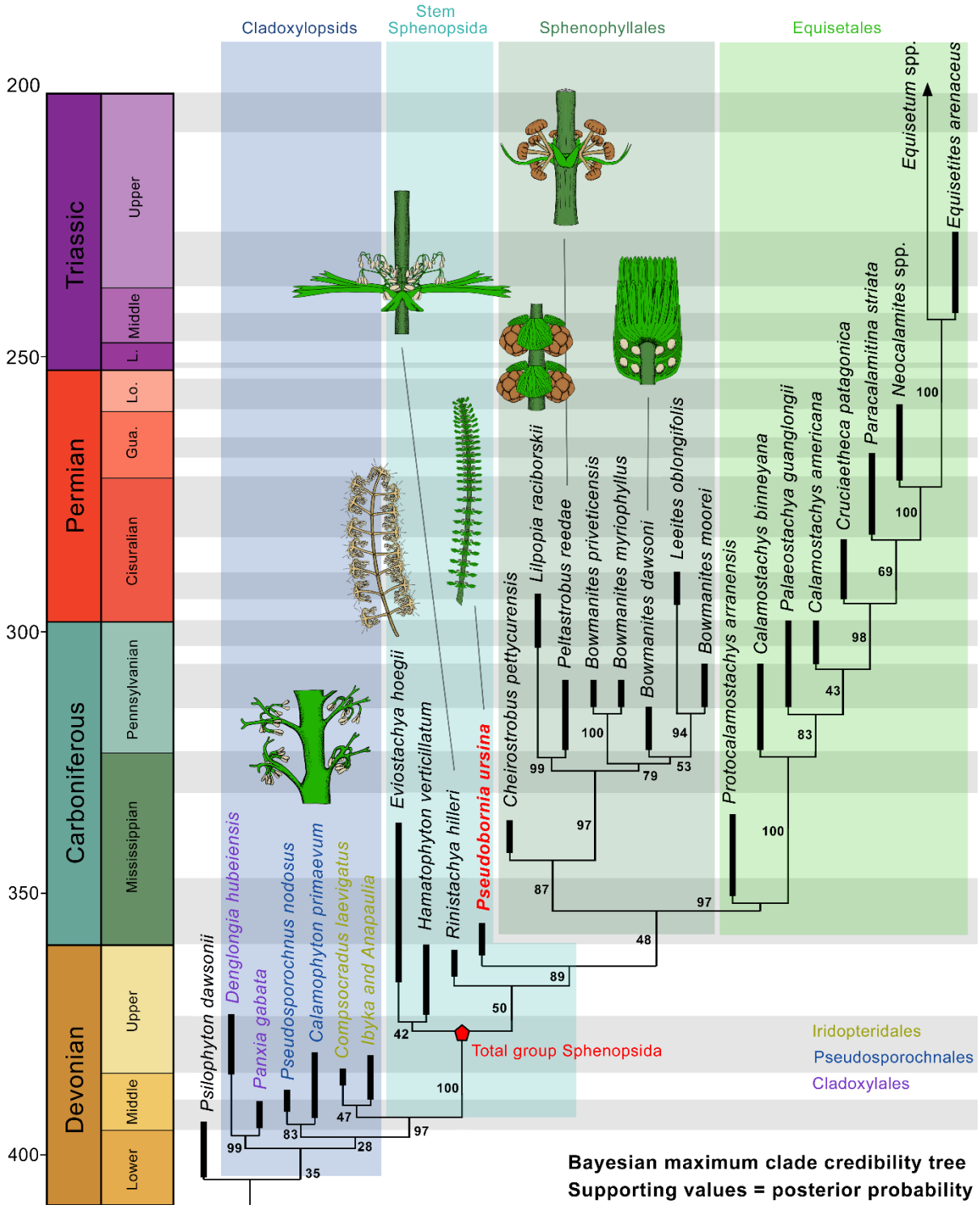

Figure 14: Time-scaled maximum clade credibility tree obtained from a Bayesian inference analysis (relaxed morphological clock). This Bayesian phylogeny is based on the same matrix of characters (Table S1) as the one used for the maximum parsimony analysis.

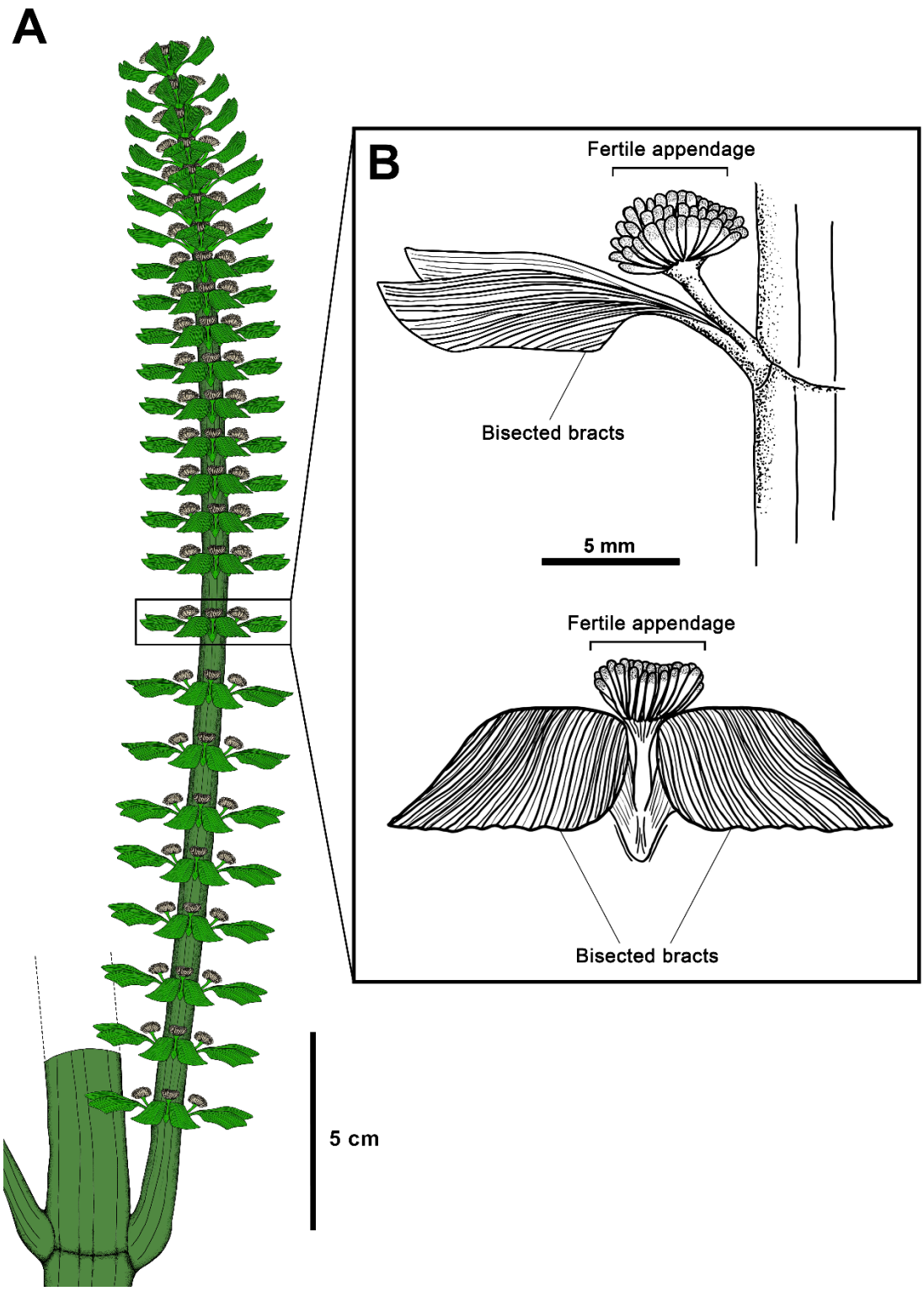

Figure 15: Suggested reconstruction of the strobilus and the fertile unit of *P. ursina*. A, Reconstructed sixth strobilus of *P. ursina*. B, Fertile unit with the bifurcated bract and its associated erected fertile appendage bearing 30 to 40 radially arranged elongated sporangia (in lateral and frontal view).

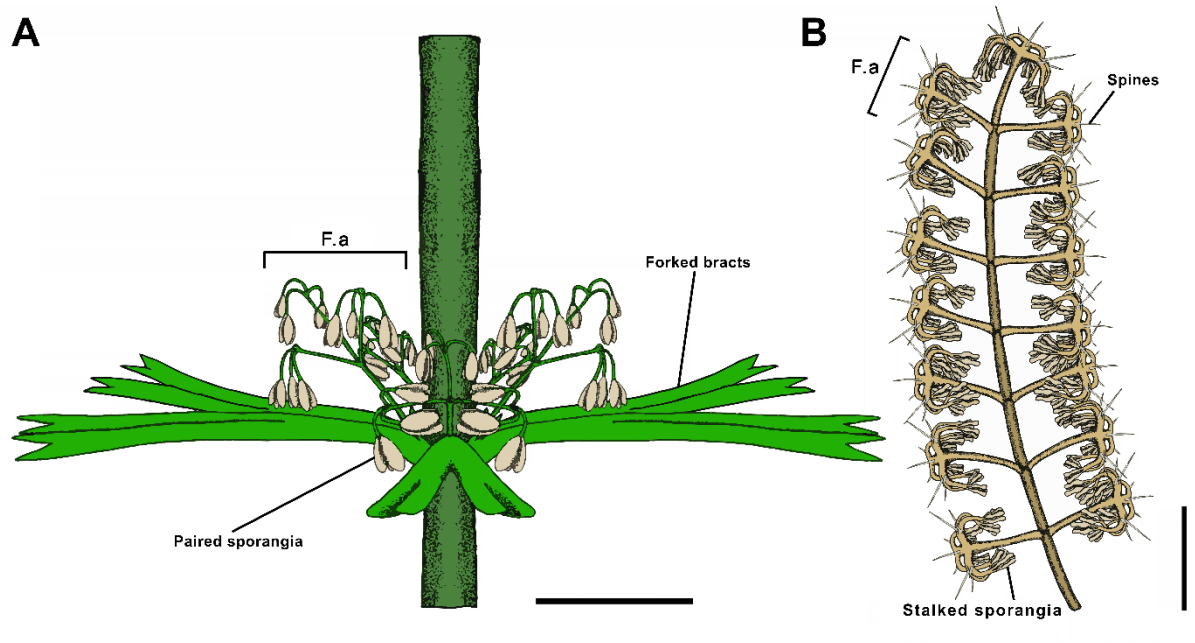

Figure 16: Reconstructions of the fertile structures of *Rinistachya hilleri* and *Eviostachya hoegi.* A, Fertile whorl of *R. hilleri* based on the specimens described by Prestianni and Gess (2019). B, Strobilus of *E. hoegi* based on the fossil described by Leclercq (1957). Scale bars = 5 mm. F.a = fertile appendage.

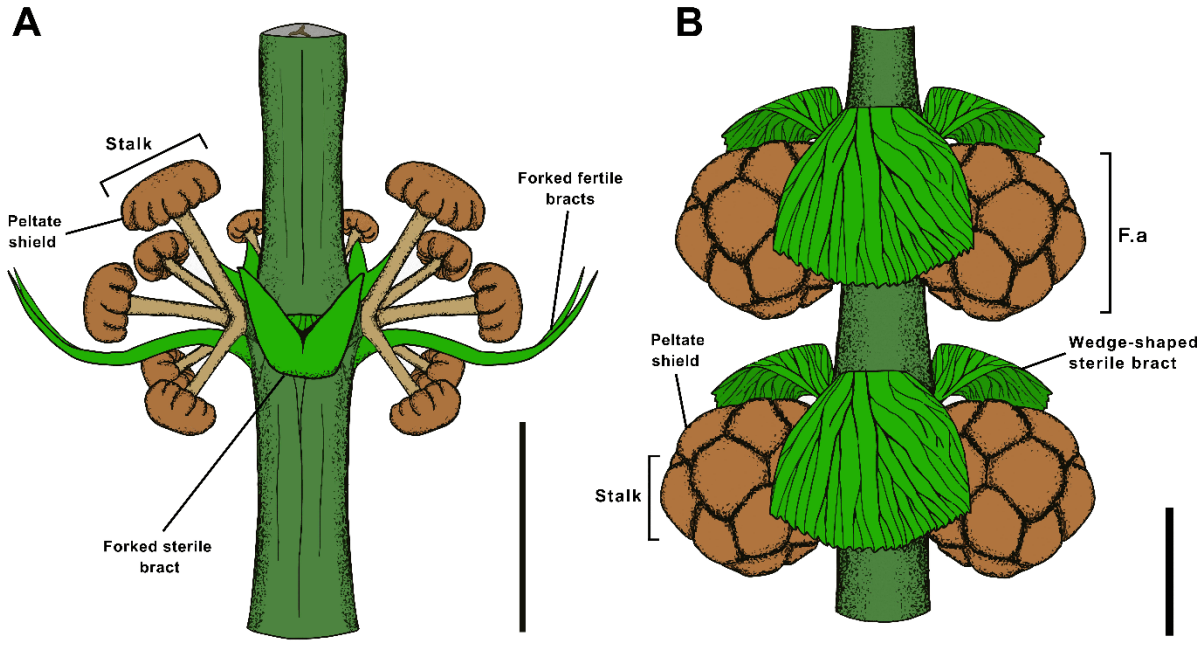

Figure 17: Reconstructions of the fertile structures of *Peltastrobus reedae* and *Lilpopia raciborskii.* A, Fertile whorl of *P. reedae* based on a permineralized specimen described and interpreted by Leisman and Graves (1964), the reconstruction is based on their interpretation. Scale bar = 2 mm. B, Two fertile whorls of *L. raciborskii* based on the re-interpretation of Kerp (1984). Scale bar = 5 mm. F.a = Fertile appendage.

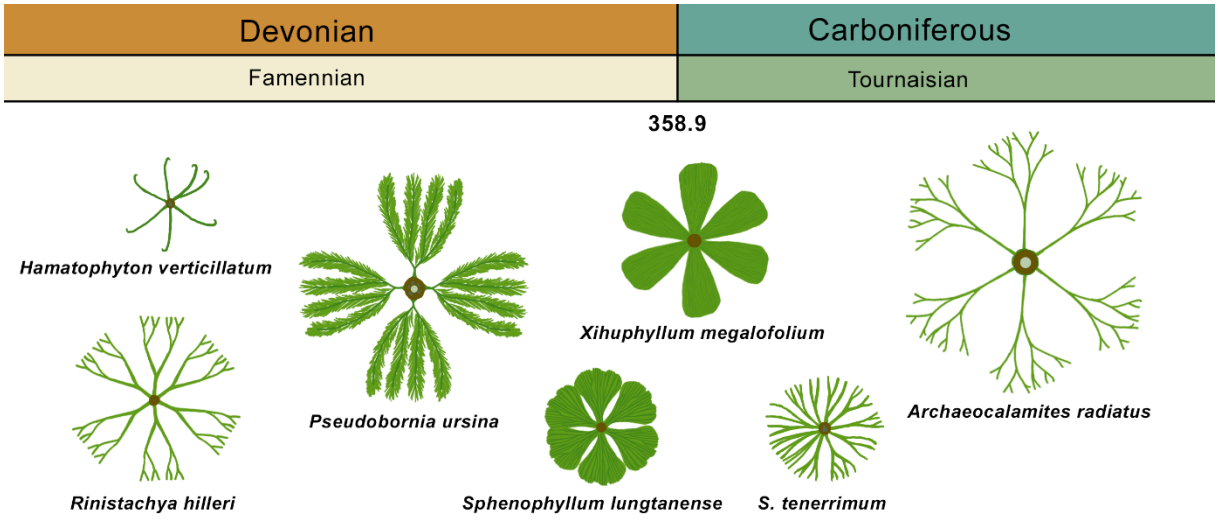

Figure 18: Reconstruction of early sphenopsid leaves from the Famennian (left) and Tournaisian (right). Irregularly divided linear leaves of *Hamatophyton verticillatum*; laciniate (=several times dichotomously divided) leaves of *Archaeocalamites radiatus* (based on Stur, 1875: pl. IV), *Pseudobornia ursina*, *Rinistachya hilleri* (Prestianni & Gess, 2019) and *Sphenophyllum tenerrimum* (based on Stur, 1877); entire and cuneate leaves of *Sphenophyllum lungtanense* and *Xihuphyllum megalofolium* (Huang *et al.*, 2017, 2022).